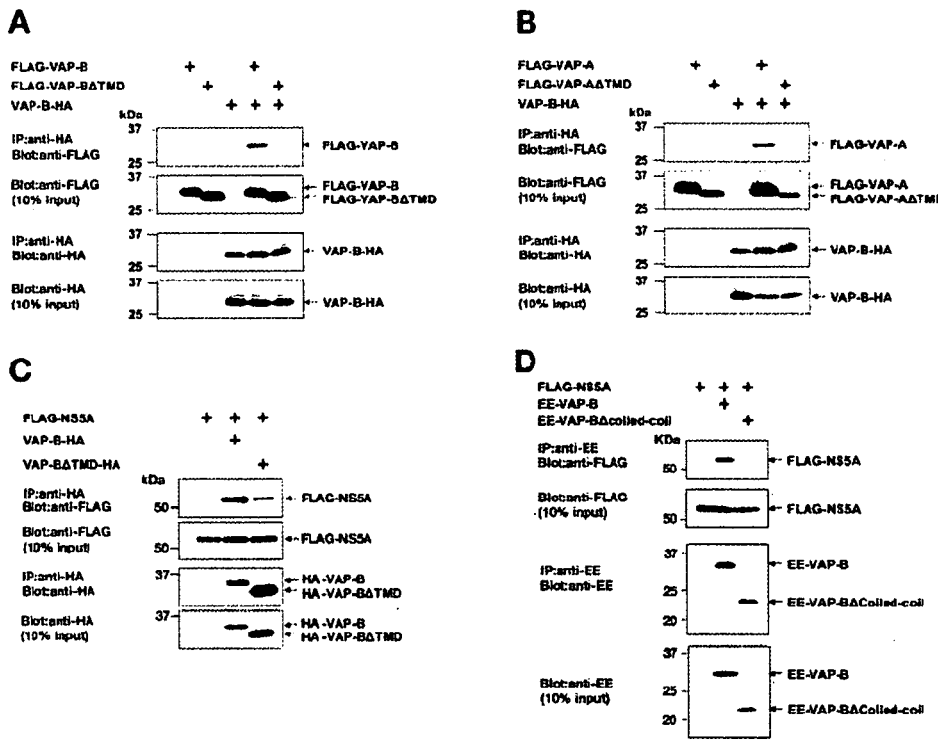


FIG. 4. VAP-B dimerizes with VAP-B and VAP-A through the TMD and interacts with NS5A via the coiled-coil domain. C-terminally HA-tagged VAP-B (VAP-B–HA) was coexpressed with FLAG–VAP-B or FLAG–VAP-B with TMD deleted (FLAG–VAP-BΔTMD). VAP-B–HA was immunoprecipitated with anti-HA antibody, and the immunoprecipitates were immunoblotted with anti-FLAG antibody (A). Interaction of VAP-B–HA with FLAG–VAP-A or FLAG–VAP-A with TMD deleted (FLAG–VAP-AΔTMD) was examined in a similar way (B). FLAG-NS5A was coexpressed with HA–VAP-B or HA–VAP-BΔTMD, and immunoprecipitates with anti-HA antibody and immunoprecipitates were immunoblotted with anti-FLAG antibody (C). FLAG-NS5A was coexpressed with EE–VAP-B or with EE–VAP-B in which the coiled-coil domain was deleted (EE–VAP-BΔcoiled-coil). EE-tagged VAP-B proteins were immunoprecipitated with anti-EE antibody, and immunoprecipitates were immunoblotted with anti-FLAG antibody (D). One-tenth of the lysates used in immunoprecipitation are shown as the 10% input. The data in each panel are representative of three independent experiments.

from amino acids 325 to 447, but not 350 to 447, exhibited binding to VAP-B, suggesting that two separate regions of NS5A (amino acids 51 to 75 and 325 to 349) are involved in physical association with VAP-B. Further mutational analyses of NS5A revealed that regions from amino acids 1 to 70, but not 1 to 65, and those from amino acids 340 to 447, but not 345 to 447, interact with VAP-B (Fig. 5B and C), suggesting that amino acids 66 to 70 and 340 to 344 are required for interaction with VAP-B. According to Tellinghuisen et al., NS5A consists of three domains, domain I (amino acids 1 to 213), domain II (amino acids 250 to 342), and domain III (amino acids 356 to 477) (46, 47). In our results, the region from amino acids 340 to 344, which is essential for the physical interaction with VAP-B, belongs to the connecting segment between domains II and III of NS5A. Ala substitution analyses revealed that an NS5A construct covering amino acids 260 to 447 that replaced the five amino acid residues between 340 and 344 with Ala abrogated interaction with VAP-B (Fig. 5D), whereas that covering 75 N-terminal amino acids carrying an Ala substitution of between 66 and 70 residues retained binding activity to VAP-B (data not shown). Therefore, we focused on the region between 340 and 344 to determine the amino acid residues in NS5A responsible for specific binding to VAP-B. A FLAG-tagged full-length NS5A carrying an Ala substitution between amino acid residues 340 and 344 (FLAG-NS5A/340-344A) exhibited a clear reduction of binding to EE–VAP-B compared with the authentic NS5A (Fig. 5E). To further determine the critical amino acids of NS5A responsible for specific binding to VAP-B, each amino acid between 340 and 344 of the NS5A construct covering amino acids from 260 to 447 was replaced with Ala, and the effect of each substitution on the interaction with VAP-B was examined by immunoprecipitation. As summarized in Fig. 5F, the four amino acid residues 341 to 344 in the polyproline cluster region of NS5A, which are highly conserved among HCV genotypes, are suggested to be involved in the interaction with VAP-B.

**VAP-B plays an important role in HCV RNA synthesis.** To determine whether VAP-B is involved in HCV replication, cell lysates isolated from Huh-7 cells harboring a subgenomic HCV replicon were used for an in vitro RNA synthesis assay. Chicken anti-human VAP-B antibody raised against synthesized peptides specifically detected endogenous and overexpressed VAP-B (Fig. 6A). Cytoplasmic fraction from the HCV replicon was added to an assay mixture containing [$\alpha$-$^{32}$P]CTP and incubated at 30°C for 4 h in the presence or absence of antibodies. Labeled RNA was analyzed by 1% formaldehyde agarose gel electrophoresis as described previously (2). Replication of the subgenomic HCV RNA was inhibited by the

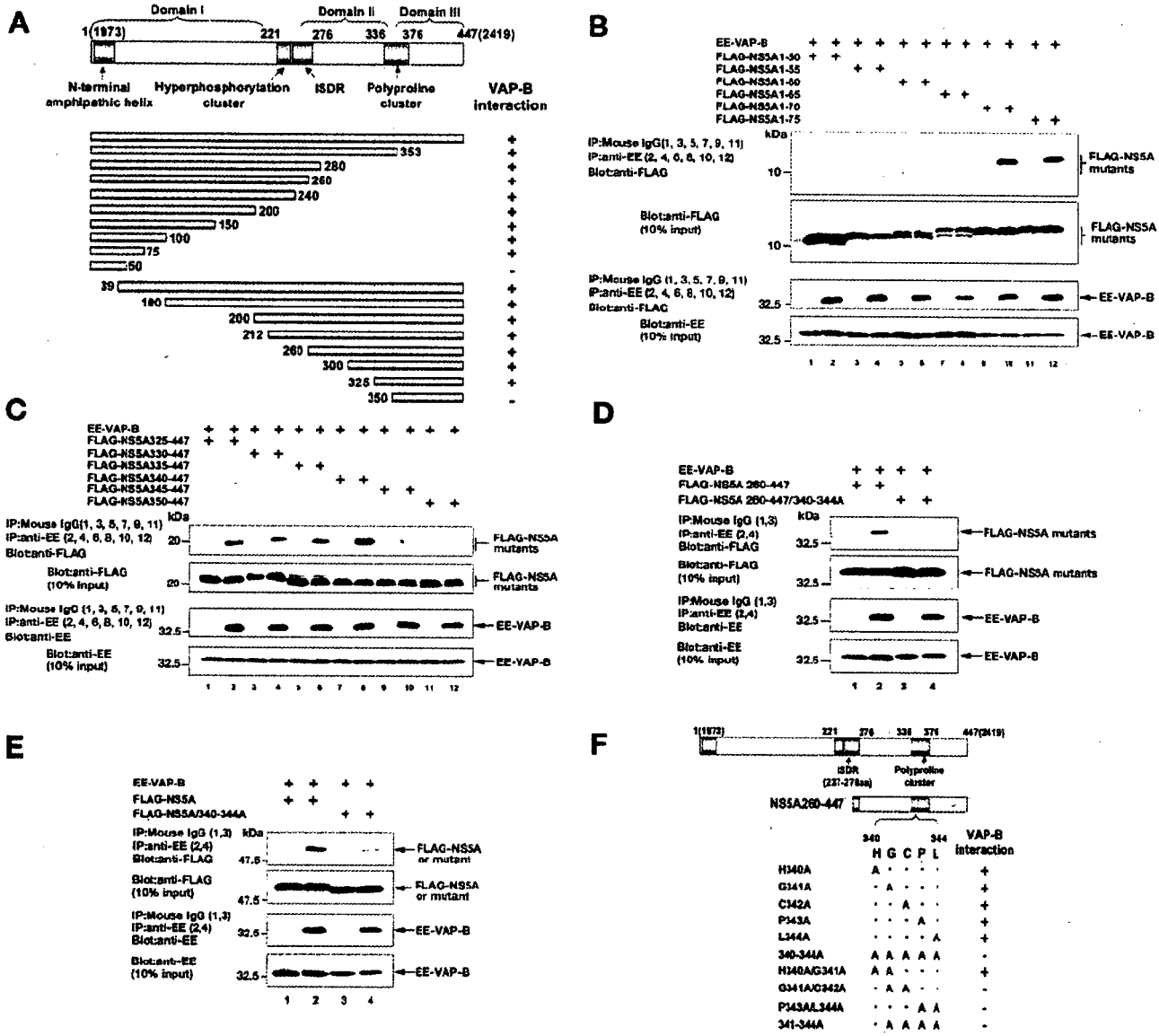


FIG. 5. Two regions of NS5A are required for VAP-B binding. N-terminal or C-terminal deletion mutants of NS5A were introduced into pEF-FLAG pGBK puro vector and coexpressed with EE–VAP-B. EE–VAP-B was immunoprecipitated with anti-EE antibody, and immunoprecipitates were immunoblotted by anti-FLAG antibody. The reverse combination of immunoprecipitation was also examined. The results are summarized in panel A. Four functional domains in the NS5A protein and three domains based on the locations of the blocks of low-complexity sequence (46) are indicated. The numbers in parentheses indicate amino acid residues in the HCV polyprotein. To further determine the critical amino acids of NS5A for specific binding to VAP-B, deletion mutants of the N-terminal region from residues 1 to 75 (B) or those of the C-terminal region from residues 325 to 447 (C) were immunoprecipitated with EE–VAP-B. Replacement of the five residues 340 to 344 with Ala was introduced into a truncated NS5A possessing residues 260 to 447, FLAG-NS5A 260-447/340-344A (D), or full-length NS5A, FLAG-NS5A/340-(E), to examine the interaction with VAP-B. Further precise mutations were introduced into NS5A possessing residues 260 to 447. The resulting mutants were coexpressed with EE–VAP-B and immunoprecipitated as described above. The results are summarized in panel F. Four amino acids (Gly, Cys, Pro, and Leu) responsible for interaction with VAP-B are indicated by dotted squares. Plus and minus indicate binding and nonbinding, respectively (A and F). One-tenth of the lysates used in immunoprecipitation are shown as the 10% input. The data in each panel are representative of three independent experiments.

antibody to VAP-B but not by a control chicken immunoglobulin G (IgG) (Fig. 6B), suggesting that VAP-B plays a critical role in HCV replication. Aizaki et al. suggested that VAP-A sequesters NS5A at an appropriate site, such as the raft-like domain on the intracellular compartment, and that the TMD of VAP-A plays an important role in subcellular localization and dimerization (2). We demonstrated that the TMD of VAP is required for hetero- and homodimerization of VAP-A and VAP-B but not for interaction with NS5A (Fig. 4). Gao et al. indicated that a truncated VAP-A mutant lacking the TMD inhibited the association of HCV NS proteins with insoluble membrane fractions and reduced both the expression level of

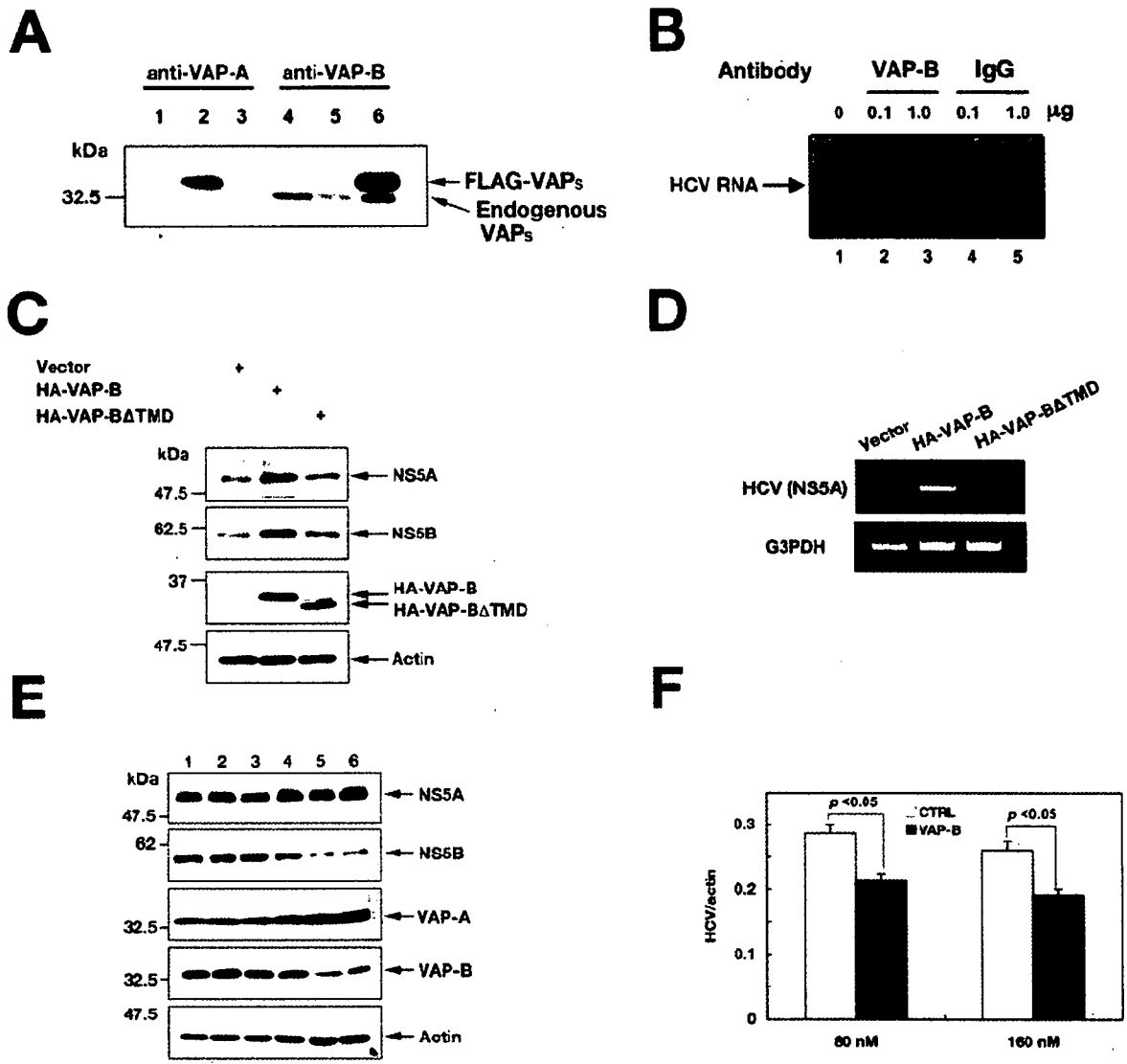


FIG. 6. VAP-B is involved in HCV replication. (A) FLAG–VAP-A (lanes 2 and 5) or FLAG–VAP-B (lanes 3 and 6) was expressed in HEK293T cells and examined by immunoblotting using anti-human VAP-A mouse monoclonal and anti-human VAP-B chicken polyclonal antibodies. (B) In vitro RNA synthesis was carried out in the presence of various concentrations of anti-human VAP-B chicken polyclonal antibody or control chicken IgG. RNA extracted from each fraction was analyzed by agarose gel electrophoresis and autoradiographed. (C) Empty plasmid, expression plasmid of N-terminally HA-tagged VAP-B (HA–VAP-B), or N-terminally HA-tagged VAP-BΔTMD (HA–VAP-BΔTMD) was transfected into HCV replicon cells. Expression of NS5A and NS5B was examined by immunoblotting. (D) HCV RNA was detected by reverse transcription-PCR using primer pairs against NS5A, and expression of G3PDH was used as a control. (E) siRNA against VAP-B or control was transfected into the HCV replicon cells. Lane 1, untreated; lane 2, treated with siFECTOR; lanes 3 and 4, control siRNA was transfected; lanes 5 and 6, VAP-B siRNA was transfected. Expression of NS5A, NS5B, VAP-A, VAP-B, and beta-actin was determined by immunoblotting at 96 h posttransfection. (F) siRNA against VAP-B or control was transfected into the HCV replicon cells. The results are expressed as standard deviations. The significance of the difference in means was determined by the Student *t* test. The data in each panel are representative of three independent experiments.

NS5A and HCV RNA replication in replicon cells (12). To determine the possible implication of VAP-B in HCV replication, VAP-B or VAP-BΔTMD was expressed in Huh-7 RNA replicon cells. In contrast with the previous data, overexpression of VAP-B increased NS5A and NS5B expression and enhanced the replication of HCV replicon cells, but no effect was observed in cells expressing VAP-BΔTMD (Fig. 6C and D). To confirm the role of VAP-B in HCV replication, we examined the effect of the knockdown of endogenous VAP-B from the HCV replicon cells by siRNA. At 96 h posttransfection, the expression of VAP-B in cells transfected with the siRNA targeted to VAP-B was reduced to half the levels of cells transfected with a control siRNA, whereas the expression of VAP-A was slightly increased. Although NS5B expression was reduced by the VAP-B knockdown, NS5A was not affected (Fig. 6E). HCV RNA

replication exhibited 25% and 27% reductions by the transfection of 80 and 160 nM siRNA, respectively, to VAP-B (Fig. 6F). Collectively, these results suggest that VAP-B plays an important role in the sequestration of NS5A and NS5B in the HCV RNA replication complex.

## DISCUSSION

Although there are conflicting data in the literature, it is accepted that NS5A is a multifunctional protein with critical roles in HCV replication, as well as in the establishment and maintenance of persistent infection (26). Tu et al. were the first to successfully isolate VAP-33 (VAP-A) as a binding partner of NS5A by a yeast two-hybrid screening of the human liver library; they also indicated an association between VAP-A and not only NS5A, but also NS5B, in mammalian cells (48). Gao et al. (12) further demonstrated that NS5A interacts with NS4B, the only HCV NS protein possessing an intrinsic ability to associate with lipid rafts; and the interaction of NS5A, NS5B, NS4B, and other NS proteins with VAP-A on lipid rafts plays a crucial role in the formation of the HCV RNA replication complex (26). Evans et al. indicated that NS5A from the Con1 strain (genotype 1b) is strongly associated with VAP-A, whereas NS5A from the H77 strain (genotype 1a) was unable to bind VAP-A in yeast (9). The determinants of subtype-specific binding to VAP-A were mapped to amino acids 2185 and 2187, and the substitution of these amino acids of the Con1 strain into those of the H77 strain abrogated both the binding to VAP-A and the replication of the subgenomic replicon. However, these defects in binding to VAP-A and in the replication of the subgenomic replicon were suppressed in the highly adaptive S2204I mutation in NS5A. The S2204I adaptive mutation was shown to disrupt NS5A hyperphosphorylation (5), and the loss of NS5A hyperphosphorylation was shown to correlate with the adaptive mutation's ability to suppress the replication defect caused by the VAP-A-noninteracting mutations (9).

To gain more insight into interaction between NS5A and host proteins involved in HCV replication, we screened human libraries by the yeast two-hybrid system using NS5A as bait and identified VAP-B as a binding protein to NS5A. VAP-B is ubiquitously expressed as VAP-A in human tissues, including liver (32). NS5A can bind to both VAP-A and VAP-B and is colocalized in intracellular compartments, such as the ER and Golgi apparatus. The coiled-coil domain of VAP-B is responsible for their interaction with NS5A, as previously reported in VAP-A (48). In the present study, two regions in NS5A are suggested to be important for VAP-B binding. One region is the N-terminal 70 residues, especially from 66 to 70 (2037 to 2042 aa in the HCV polyprotein), although replacement of these 5 residues with Ala could not abrogate binding to VAP-B. The other is identified at the C-terminal polyproline cluster, and replacement of these four residues from 341 to 344 (2313 to 2316 aa in the HCV polyprotein) with Ala in a full-length NS5A reduced VAP-B binding. Two class II polyproline motifs (consensus PXXPXR) are identified in the polyproline cluster and can bind the SH3 domains of a number of cellular signaling proteins, including Grb2 (45), amphiphysin II (56), and Src family tyrosine kinases (25). Pro343 and Leu344 in the C-terminal VAP-B binding region are part of the first class II polyproline motif. The overlapping of VAP-B's binding region with other cellular signaling proteins may suggest interplay between cellular signaling and replication of HCV. A previous observation indicated that the interaction between NS5A and VAP-A was genotype specific, and amino acid residues critical for the interaction were mapped to amino acids 2185 and 2187 in yeast (9). However, the same authors indicated that NS5A derived from either the1a or 1b genotype expressed in Huh-7 cells interacted equally well with a glutathione *S*-transferase fusion VAP-A expressed in bacteria in vitro, and an attempt at selective interaction of hypophosphorylated NS5A from replicon cells with VAP-A was not successful (9). Furthermore, in our study, no clear difference was detected between native NS5A and the S2204I mutant in binding to VAP-A or VAP-B by immunoprecipitation analyses in mammalian cells (data not shown). In addition, the data in Fig. 2 clearly indicate that NS5A genotype 1a binds to both VAP-A and VAP-B, even though this genotype carries the VAP-A-noninteracting mutations (A2185 and G2187). This discrepancy might be explained by the differences between the experimental systems, including the condition of cell lines, the intracellular ratio of VAP-A and VAP-B, and the phosphorylation status of NS5A. Evans et al. proposed that hyperphosphorylated p58 NS5A represents a closed conformation that cannot interact with VAP-A, whereas hypophosphorylated p56 NS5A represents an open conformation capable of strong interaction with VAP-A (9). The phosphorylation of NS5A is a critical modification that controls not only its interaction with VAP-A, but also RNA replication in Huh7 replicon cells (9, 31). Further study will be needed to elucidate the relationship between the phosphorylation status of NS5A and the capability of binding to VAP-B.

The inhibition of HCV RNA replication by the specific antibody to VAP-B in vitro indicated that VAP-B is a component of the HCV RNA replication complex. Furthermore, the reduction of VAP-B expression by siRNA induced the suppression of NS5B expression but not of NS5A, as seen in the knockdown experiment with VAP-A (12). This suggested that VAP plays an important role in the participation of NS5B in the replication complex. VAP could form hetero- and homodimers through their TMDs and interact with NS5A through their coiled-coil domains (Fig. 4). VAP-C is a splicing variant of VAP-B missing 60% of the C terminus. Therefore, VAP-C cannot interact with VAP-A, VAP-B, or NS5A. Although it is difficult to determine precisely the participation of the monomer and dimer of VAP-A and VAP-B in the HCV replication complex, it might be plausible to speculate that VAP-A is expressed more abundantly than VAP-B and that the heterodimer of VAP-A and VAP-B is more active as an HCV replication complex than those of the monomeric or homodimeric forms. Therefore, overexpression of VAP-B, but not of VAP-A, enhanced HCV RNA replication by providing scaffolds in appropriate positions, like the raft-like domain in the ER/Golgi compartment, capable of changing the nonfunctional NS proteins into a replication-competent state, because only a small fraction of NS proteins are functional as replication complexes (20, 28). Furthermore, VAP-A might have a higher affinity to NS5B than VAP-B does, and overexpression of the TMD deletion mutant of VAP-A, but not that of VAP-B, exhibited a reduction of RNA replication (12). The

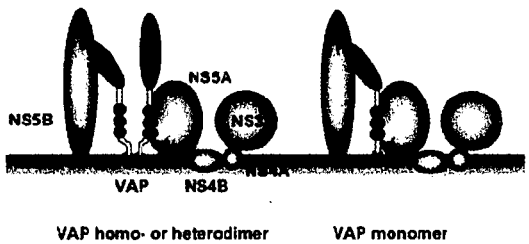


FIG. 7. Models of interaction between HCV NS proteins and VAP. Monomeric and hetero- or homodimeric forms of VAPs can interact with NS5A and NS5B through the coiled-coil domain and N-terminal region, respectively. NS4B can associate with lipid rafts and interact with NS5A (9). NS4A is a cofactor of NS3 and recruits NS3 to the HCV NS protein complex.

possible implication of monomeric and dimeric forms of VAPs in the replication complex of HCV is shown in Fig. 7.

In this study, we identified VAP-B as a novel binding protein to NS5A and NS5B and demonstrated its participation in HCV RNA replication. Elucidation of the precise roles of VAP-A and VAP-B in the phosphorylation of NS5A and in the formation of the replication complex through interaction with other HCV NS proteins and host proteins should provide clues to understanding the molecular mechanisms underlying the replication of HCV RNA and to developing novel therapeutics for chronic hepatitis C.

## ACKNOWLEDGMENTS

We thank H. Murase for secretarial work. We also thank R. Bartenschlager, J. Bukh, and D. C. S. Huang for giving us replicon cells, the HCV H77 clone, and plasmids, respectively.

This work was supported in part by grants-in-aid from the Ministry of Health, Labor, and Welfare; the Ministry of Education, Culture, Sports, Science, and Technology; the Program for Promotion of Fundamental Studies in Health Science of the National Institute of Biomedical Innovation (NIBIO); the 21st Century Center of Excellence Program; and the Foundation for Biomedical Research and Innovation.

## REFERENCES

1. Aizaki, H., Y. Aoki, T. Harada, K. Ishii, T. Suzuki, S. Nagamori, G. Toda, Y. Matsuura, and T. Miyamura. 1998. Full-length complementary DNA of hepatitis C virus genome from an infectious blood sample. Hepatology 27: 621–627.
2. Aizaki, H., K. Lee, V. M.-H. Sung, H. Ishiki, and M. M. C. Lai. 2004. Characterization of the hepatitis C virus RNA replication complex associated with lipid rafts. Virology 324:450–461.
3. Ali, N., K. D. Tardif, and A. Siddiqui. 2002. Cell-free replication of the hepatitis C virus subgenomic replicon. J. Virol. 76:12001–12007.
4. Appel, N., T. Pietschmann, and R. Bartenschlager. 2005. Mutational analysis of hepatitis C virus nonstructural protein 5A: potential role of differential phosphorylation in RNA replication and identification of a genetically flexible domain. J. Virol. 79:3187–3194.
5. Blight, K. J., J. A. McKeating, J. Marcotrigiano, and C. M. Rice. 2003. Efficient replication of hepatitis C virus genotype 1a RNAs in cell culture. J. Virol. 77:3181–3190.
6. Cerny, A., and F. V. Chisari. 1999. Pathogenesis of chronic hepatitis C: immunological features of hepatic injury and viral persistence. Hepatology 30:595–601.
7. Christopher, V., N. Scolding, and R. T. Przemioslo. 2005. Acute hepatitis secondary to interferon beta-1a in multiple sclerosis. J. Neurol. 252:855–856.
8. Chung, K. M., J. Lee, J. E. Kim, O. K. Song, S. Cho, J. Lim, M. Seedorf, B. Hahm, and S. K. Jang. 2000. Nonstructural protein 5A of hepatitis C virus inhibits the function of karyopherin β3. J. Virol. 74:5233–5241.
9. Evans, M. J., C. M. Rice, and S. P. Goff. 2004. Phosphorylation of hepatitis C virus nonstructural protein 5A modulates its protein interactions and viral RNA replication. Proc. Natl. Acad. Sci. USA 101:13038–13043.
10. Foster, L. J., M. L. Weir, D. Y. Lim, Z. Liu, W. S. Trimble, and A. Klip. 2000. A functional role for VAP-33 in insulin-stimulated GLUT4 traffic. Traffic 1:512–521.
11. Gale, M. J., Jr., M. J. Korth, N. M. Tang, S. L. Tan, D. A. Hopkins, T. E. Dever, S. J. Polyak, D. R. Gretch, and M. G. Katze. 1997. Evidence that hepatitis C virus resistance to interferon is mediated through repression of the PKR protein kinase by the nonstructural 5A protein. Virology 230:217–227.
12. Gao, L., H. Aizaki, J. W. He, and M. M. Lai. 2004. Interactions between viral nonstructural proteins and host protein hVAP-33 mediate the formation of hepatitis C virus RNA replication complex on lipid raft. J. Virol. 78:3480–3488.
13. Girod, A., B. Storrie, J. C. Simpson, L. Johannes, B. Goud, L. M. Roberts, J. M. Lord, T. Nilsson, and R. Pepperkok. 1999. Evidence for a COP-I-independent transport route from the Golgi complex to the endoplasmic reticulum. Nat. Cell Biol. 1:423–430.
14. Hardy, R. W., J. Marcotrigiano, K. J. Blight, J. E. Majors, and C. M. Rice. 2003. Hepatitis C virus RNA synthesis in a cell-free system isolated from replicon-containing hepatoma cells. J. Virol. 77:2029–2037.
15. He, Y., H. Nakao, S. L. Tan, S. J. Polyak, P. Neddermann, S. Vijaysri, B. L. Jacobs, and M. G. Katze. 2002. Subversion of cell signaling pathways by hepatitis C virus nonstructural 5A protein via interaction with Grb2 and P85 phosphatidylinositol 3-kinase. J. Virol. 76:9207–9217.
16. Ho, S. N., H. D. Hunt, R. M. Horton, J. K. Pullen, and L. R. Pease. 1989. Site-directed mutagenesis by overlap extension using the polymerase chain reaction. Gene 77:51–59.
17. Horton, R. M., H. D. Hunt, S. N. Ho, J. K. Pullen, and L. R. Pease. 1989. Engineering hybrid genes without the use of restriction enzymes: gene splicing by overlap extension. Gene 77:61–68.
18. Huang, D. C., S. Cory, and A. Strasser. 1997. Bcl-2, Bcl-XL and adenovirus protein E1B19kD are functionally equivalent in their ability to inhibit cell death. Oncogene 14:405–414.
19. Kapadia, S. B., and F. V. Chisari. 2005. Hepatitis C virus RNA replication is regulated by host geranylgeranylation and fatty acids. Proc. Natl. Acad. Sci. USA 102:2561–2566.
20. Kishine, H., K. Sugiyama, M. Hijikata, N. Kato, H. Takahashi, T. Noshi, Y. Nio, M. Hosaka, Y. Miyanari, and K. Shimotohno. 2002. Subgenomic replicon derived from a cell line infected with the hepatitis C virus. Biochem. Biophys. Res. Commun. 293:993–999.
21. Koch, J. O., and R. Bartenschlager. 1999. Modulation of hepatitis C virus NS5A hyperphosphorylation by nonstructural proteins NS3, NS4A, and NS4B. J. Virol. 73:7138–7146.
22. Lapierre, L. A., P. L. Tuma, J. Navarre, J. R. Goldenring, and J. M. Anderson. 1999. VAP-33 localizes to both an intracellular vesicle population and with occludin at the tight junction. J. Cell Sci. 112:3723–3732.
23. Loewen, C. J., and T. P. Levine. 2005. A highly conserved binding site in VAP for the FFAT motif of lipid binding proteins. J. Biol. Chem. 280:14097–14104.
24. Lohmann, V., F. Korner, J. Koch, U. Herian, L. Theilmann, and R. Bartenschlager. 1999. Replication of subgenomic hepatitis C virus RNAs in a hepatoma cell line. Science 285:110–113.
25. Macdonald, A., K. Crowder, A. Street, C. McCormick, and M. Harris. 2004. The hepatitis C virus NS5A protein binds to members of the Src family of tyrosine kinases and regulates kinase activity. J. Gen. Virol. 85:721–729.
26. Macdonald, A., and M. Harris. 2004. Hepatitis C virus NS5A: tales of a promiscuous protein. J. Gen. Virol. 85:2485–2502.
27. Majumder, M., A. K. Ghosh, R. Steele, R. Ray, and R. B. Ray. 2001. Hepatitis C virus NS5A physically associates with p53 and regulates p21/waf1 gene expression in a p53-dependent manner. J. Virol. 75:1401–1407.
28. Miyanari, Y., M. Hijikata, M. Yamaji, M. Hosaka, H. Takahashi, and K. Shimotohno. 2003. Hepatitis C virus non-structural proteins in the probable membranous compartment function in viral genome replication. J. Biol. Chem. 278:50301–50308.
29. Moriishi, K., and Y. Matsuura. 2003. Mechanisms of hepatitis C virus infection. Antivir. Chem. Chemother. 14:285–297.
30. Neddermann, P., A. Clementi, and R. De Francesco. 1999. Hyperphosphorylation of the hepatitis C virus NS5A protein requires an active NS3 protease, NS4A, NS4B, and NS5A encoded on the same polyprotein. J. Virol. 73:9984–9991.
31. Neddermann, P., M. Quintavalle, C. Di Pietro, A. Clementi, M. Cerretani, S. Altamura, L. Bartholomew, and R. De Francesco. 2004. Reduction of hepatitis C virus NS5A hyperphosphorylation by selective inhibition of cellular kinases activates viral RNA replication in cell culture. J. Virol. 78:13306–13314.
32. Nishimura, Y., M. Hayashi, H. Inada, and T. Tanaka. 1999. Molecular cloning and characterization of mammalian homologues of vesicle-associated membrane protein-associated (VAMP-associated) proteins. Biochem. Biophys. Res. Commun. 254:21–26.
33. Niwa, H., K. Yamamura, and J. Miyazaki. 1991. Efficient selection for high-expression transfectants with a novel eukaryotic vector. Gene 108:193–199.
34. O'Connor, L., A. Strasser, L. A. O'Reilly, G. Hausmann, J. M. Adams, S.

Cory, and D. C. Huang. 1998. Bim: a novel member of the Bcl-2 family that promotes apoptosis. EMBO J. 17:384–395.
35. Pawlotsky, J. M., and G. Germanidis. 1999. The non-structural 5A protein of hepatitis C virus. J. Viral. Hepat. 6:343–356.
36. Pietschmann, T., V. Lohmann, G. Rutter, K. Kurpanek, and R. Bartenschlager. 2001. Characterization of cell lines carrying self-replicating hepatitis C virus RNAs. J. Virol. 75:1252–1264.
37. Qadri, I., M. Iwahashi, and F. Simon. 2002. Hepatitis C virus NS5A protein binds TBP and p53, inhibiting their DNA binding and p53 interactions with TBP and ERCC3. Biochim. Biophys. Acta 1592:193–204.
38. Schoch, S., F. Deak, A. Konigstorfer, M. Mozhayeva, Y. Sara, T. C. Sudhof, and E. T. Kavalali. 2001. SNARE function analyzed in synaptobrevin/VAMP knockout mice. Science 294:1117–1122.
39. Shi, S. T., K. J. Lee, H. Aizaki, S. B. Hwang, and M. M. Lai. 2003. Hepatitis C virus RNA replication occurs on a detergent-resistant membrane that cofractionates with caveolin-2. J. Virol. 77:4160–4168.
40. Shi, S. T., S. J. Polyak, H. Tu, D. R. Taylor, D. R. Gretch, and M. M. Lai. 2002. Hepatitis C virus NS5A colocalizes with the core protein on lipid droplets and interacts with apolipoproteins. Virology 292:198–210.
41. Shimakami, T., M. Hijikata, H. Luo, Y. Y. Ma, S. Kaneko, K. Shimotohno, and S. Murakami. 2004. Effect of interaction between hepatitis C virus NS5A and NS5B on hepatitis C virus RNA replication with the hepatitis C virus replicon. J. Virol. 78:2738–2748.
42. Skehel, P. A., R. Fabian-Fine, and E. R. Kandel. 2000. Mouse VAP33 is associated with the endoplasmic reticulum and microtubules. Proc. Natl. Acad. Sci. USA 97:1101–1106.
43. Skehel, P. A., K. C. Martin, E. R. Kandel, and D. Bartsch. 1995. A VAMP-binding protein from Aplysia required for neurotransmitter release. Science 269:1580–1583.
44. Soussan, L., D. Burakov, M. P. Daniels, M. Toister-Achituv, A. Porat, Y. Yarden, and Z. Elazar. 1999. ERG30, a VAP-33-related protein, functions in protein transport mediated by COPI vesicles. J. Cell Biol. 146:301–311.
45. Tan, S. L., H. Nakao, Y. He, S. Vijaysri, P. Neddermann, B. L. Jacobs, B. J. Mayer, and M. G. Katze. 1999. NS5A, a nonstructural protein of hepatitis C virus, binds growth factor receptor-bound protein 2 adaptor protein in a Src homology 3 domain/ligand-dependent manner and perturbs mitogenic signaling. Proc. Natl. Acad. Sci. USA 96:5533–5538.
46. Tellinghuisen, T. L., J. Marcotrigiano, A. E. Gorbalenya, and C. M. Rice. 2004. The NS5A protein of hepatitis C virus is a zinc metalloprotein. J. Biol. Chem. 279:48576–48587.
47. Tellinghuisen, T. L., J. Marcotrigiano, and C. M. Rice. 2005. Structure of the zinc-binding domain of an essential component of the hepatitis C virus replicase. Nature 435:374–379.
48. Tu, H., L. Gao, S. T. Shi, D. R. Taylor, T. Yang, A. K. Mircheff, Y. Wen, A. E. Gorbalenya, S. B. Hwang, and M. M. Lai. 1999. Hepatitis C virus RNA polymerase and NS5A complex with a SNARE-like protein. Virology 263: 30–41.
49. Wang, C., M. Gale, Jr., B. C. Keller, H. Huang, M. S. Brown, J. L. Goldstein, and J. Ye. 2005. Identification of FBL2 as a geranylgeranylated cellular protein required for hepatitis C virus RNA replication. Mol. Cell 18:425–434.
50. Weir, M. L., A. Klip, and W. S. Trimble. 1998. Identification of a human homologue of the vesicle-associated membrane protein (VAMP)-associated protein of 33 kDa (VAP-33): a broadly expressed protein that binds to VAMP. Biochem. J. 333:247–251.
51. Weir, M. L., H. Xie, A. Klip, and W. S. Trimble. 2001. VAP-A binds promiscuously to both v- and tSNAREs. Biochem. Biophys. Res. Commun. 286:616–621.
52. Yanagi, M., R. H. Purcell, S. U. Emerson, and J. Bukh. 1997. Transcripts from a single full-length cDNA clone of hepatitis C virus are infectious when directly transfected into the liver of a chimpanzee. Proc. Natl. Acad. Sci. USA 94:8738–8743.
53. Yang, G., D. C. Pevear, M. S. Collett, S. Chunduru, D. C. Young, C. Benetatos, and R. Jordan. 2004. Newly synthesized hepatitis C virus replicon RNA is protected from nuclease activity by a protease-sensitive factor(s). J. Virol. 78:10202–10205.
54. Ye, J., C. Wang, R. Sumpter, Jr., M. S. Brown, J. L. Goldstein, and M. Gale, Jr. 2003. Disruption of hepatitis C virus RNA replication through inhibition of host protein geranylgeranylation. Proc. Natl. Acad. Sci. USA 100:15865–15870.
55. Yi, M., and S. M. Lemon. 2004. Adaptive mutations producing efficient replication of genotype 1a hepatitis C virus RNA in normal Huh7 cells. J. Virol. 78:7904–7915.
56. Zech, B., A. Kurtenbach, N. Krieger, D. Strand, S. Blencke, M. Morbitzer, K. Salassidis, M. Cotten, J. Wissing, S. Obert, R. Bartenschlager, T. Herget, and H. Daub. 2003. Identification and characterization of amphiphysin II as a novel cellular interaction partner of the hepatitis C virus NS5A protein. J. Gen. Virol. 84:555–560.

JOURNAL OF VIROLOGY, Mar. 2005, p. 3448–3458 Vol. 79, No. 6
0022-538X/05/$08.00+0 doi:10.1128/JVI.79.6.3448–3458.2005


# Nuclear Localization of Japanese Encephalitis Virus Core Protein Enhances Viral Replication†

Yoshio Mori,[1] Tamaki Okabayashi,[1] Tetsuo Yamashita,[1] Zijiang Zhao,[2] Takaji Wakita,[2] Kotaro Yasui,[2] Futoshi Hasebe,[3] Masayuki Tadano,[4] Eiji Konishi,[5] Kohji Moriishi,[1] and Yoshiharu Matsuura[1]*

*Research Center for Emerging Infectious Diseases, Research Institute for Microbial Diseases, Osaka University, Osaka,[1] Department of Microbiology, Tokyo Metropolitan Institute for Neuroscience, Tokyo,[2] Department of Virology, Institute of Tropical Medicine, Nagasaki University, Nagasaki,[3] Division of Molecular Virology and Oncology, University of the Ryukyu, Okinawa,[4] Department of Health Sciences, Kobe University School of Medicine, Hyogo,[5] Japan*

Received 13 September 2004/Accepted 3 November 2004

**Japanese encephalitis virus (JEV) core protein was detected in both the nucleoli and cytoplasm of mammalian and insect cell lines infected with JEV or transfected with the expression plasmid of the core protein. Mutation analysis revealed that $Gly^{42}$ and $Pro^{43}$ in the core protein are essential for the nuclear and nucleolar localization. A mutant M4243 virus in which both $Gly^{42}$ and $Pro^{43}$ were replaced by Ala was recovered by plasmid-based reverse genetics. In C6/36 mosquito cells, the M4243 virus exhibited RNA replication and protein synthesis comparable to wild-type JEV, whereas propagation in Vero cells was impaired. The mutant core protein was detected in the cytoplasm but not in the nucleus of either C6/36 or Vero cell lines infected with the M4243 virus. The impaired propagation of M4243 in mammalian cells was recovered by the expression of wild-type core protein in *trans* but not by that of the mutant core protein. Although M4243 mutant virus exhibited a high level of neurovirulence comparable to wild-type JEV in spite of the approximately 100-fold-lower viral propagation after intracerebral inoculation to 3-week-old mice of strain Jcl:ICR, no virus was recovered from the brain after intraperitoneal inoculation of the mutant. These results indicate that nuclear localization of JEV core protein plays crucial roles not only in the replication in mammalian cells in vitro but also in the pathogenesis of encephalitis induced by JEV in vivo.**

*Japanese encephalitis virus* (JEV) belongs to the genus *Flavivirus* within the family *Flaviviridae*. Members of the genus *Flavivirus* are predominantly arthropodborne viruses and frequently cause significant morbidity and mortality in mammals and birds (6). JEV is distributed in the south and southeast regions of Asia and kept in a zoonotic transmission cycle between pigs or birds and mosquitoes (6, 50, 57). JEV spreads to dead-end hosts, including humans, through the bite of JEV-infected mosquitoes and causes infection of the central nervous system, with a high mortality rate (6, 57). JEV has a single-stranded positive-strand RNA genome approximately 11 kb in length, which is capped at the 5′ end but lacks modification of the 3′ terminus by polyadenylation (34). The genomic RNA encodes a single large open reading frame, and a polyprotein translated from the genome is cleaved co- and posttranslationally by host and viral proteases to yield three structural proteins, the core, precursor membrane (prM), and envelope (E) proteins, and seven nonstructural proteins, NS1, NS2A, NS2B, NS3, NS4A, NS4B, and NS5 (53). Although the core protein has very little amino acid homology to other flaviviruses—for example, the core protein of JEV has only 25% homology to that of tick-borne encephalitis virus (TBEV)—the structural properties, such as the hydrophobicity profile, abundances of basic amino acid residues, and secondary structures, are very similar (11, 20, 36). The flavivirus core proteins commonly contain two hydrophobic sequences in the center and a carboxyl-terminal end, and the carboxyl-terminal hydrophobic region serves as a signal sequence of prM. The signal-anchor sequence is cleaved off by the viral protease NS2B-3, and this cleavage is required for the subsequent liberation of the amino terminus of prM by the host signal peptidase (35, 52, 63). The mature core protein, released from the endoplasmic reticulum (ER) membrane, is believed to bind to the genomic RNA via the basic amino acid clusters at the amino and carboxyl termini and forms nucleocapsids (23). The central hydrophobic region of the core protein may be associated with the ER membrane, and this interaction is believed to facilitate the assembly of nucleocapsid and two membrane proteins, prM and E, and to bud into the ER lumen as virions (39). The removal of the central hydrophobic region of the TBEV core protein increased the production of the subviral particles that consist of (pr)M and E proteins but that lack a core protein and genomic RNA (26, 27).

In addition to their role as structural proteins, core proteins of dengue virus (DEN) and Kunjin virus (KUN) are localized not only in the cytoplasm but also in the nucleus, especially in the nucleoli of several infected cell lines (4, 38, 55, 59, 61). Transport from the cytoplasm to the nucleus occurs through nuclear pore complexes that penetrate the double lipid layers of the nuclear envelope. Small molecules up to 9 nm in diameter (<50 kDa) can freely diffuse through the nuclear pore complexes, while most macromolecules require an active transport process via nuclear import receptor proteins such as impotin-α (37). In general, cargo proteins contain mono- or bi-

* Corresponding author. Mailing address: Research Center for Emerging Infectious Diseases, Research Institute for Microbial Diseases, Osaka University, 3-1 Yamada-oka, Suita, Osaka 565-0871, Japan. Phone: 81-6-6879-8340. Fax: 81-6-6879-8269. E-mail: matsuura@biken.osaka-u.ac.jp.

† This study is dedicated to the memory of Ikuko Yanase.

partite cluster sequences of basic amino acids termed nuclear localization signals (NLSs) to bind to nuclear import receptor proteins (5, 21). As flavivirus core proteins are relatively small (approximately 14 kDa), they may diffuse into the nucleus. However, the successful translocation of DEN core protein fused with three copies of green fluorescent protein (GFP) (96 kDa in total) into the nucleus indicates that the DEN core protein is actively translocated into the nucleus by an energy-dependent pathway, and an NLS was assigned to the region of carboxyl-terminal residues from amino acids 85 to 100 (59). Despite the many studies investigating this matter, the biological significance of the nuclear localization of core proteins in the virus replication cycle remains unclear.

In this study, we showed that the JEV core protein is also localized in both the cytoplasm and the nucleus, particularly in the nucleolus, of mammalian and mosquito cell lines and determined that an NLS is present in the core protein. We generated a mutant JEV, replaced the NLS in the core protein with Ala, and confirmed the elimination of the nuclear localization of the mutant core protein in both mammalian and mosquito cells. The characterization of the mutant JEV indicates that the nuclear localization of the core protein plays important roles in the viral replication in mammalian cells and in the pathogenesis of encephalitis in vivo. Finally, we discuss the biological significance of the nuclear localization of the JEV core protein.

## MATERIALS AND METHODS

**Cells.** The mammalian cell lines Vero (African green monkey kidney), 293T (human kidney), BHK (hamster kidney), HeLa (human cervix cancer), HepG2 (human hepatoma), SK-N-SH (human neuroblastoma), and N18 (mouse neuroblastoma) were maintained in Dulbecco's modified Eagle's minimal essential medium (D-MEM) supplemented with 10% fetal bovine serum (FBS). A mosquito cell line, C6/36 (*Aedes albopictus*), was grown in Eagle's minimal essential medium supplemented with 10% FBS.

**Plasmids.** The mammalian expression vector pEGFP-C3 was purchased from Clontech (Palo Alto, Calif.). The plasmid pEGFP-JEVC105 was constructed by insertion of cDNA encoding the mature form of the JEV core protein without the C-terminal signal sequence (amino acids 2 to 105 of the AT31 strain) amplified by PCR into pEGFP-C3 as described previously (42). All of the expression vectors coding the enhanced GFP (EGFP)-fused mutant JEV core proteins were constructed based on pEGFP-JEVC105. Briefly, the gene encoding the JEV core protein with amino acids 38 to 44 deleted was amplified by splicing the overlapping extension (16, 17). For alanine scanning in putative NLS regions (amino acids 38 to 44 and 85 to 105), a series of point mutants of the JEV core protein were synthesized by PCR-based mutagenesis (14). All of the mutant genes were cloned into EcoRI and BamHI sites of pEGFP-C3. The plasmid that has a full-length cDNA of the JEV AT31 strain under the control of a T7 promoter was constructed and designated pMWJEATG1 (Z. Zhao, T. Date, Y. Li, T. Kato, M. Miyamoto, K. Yasui, and T. Wakita, submitted for publication). Guanine-to-cytosine and cytosine-to-guanine point mutations were introduced into pMWJEATG1 at nucleotides 220 and 222 of the JEV gene, respectively, by PCR-based mutagenesis to change $Gly^{42}$ and $Pro^{43}$ of the core protein to Ala. The constructed plasmid was designated pMWJEAT/GP4243AA. For the mutant viral replication complementation experiments, the genes coding the C-terminal hemagglutinin (HA)-tagged core proteins derived from pMWJEATG1 and pMWJEAT/GP4243AA were cloned into pCAG-GS vector (43), and the resulting plasmids were designated pCAG-WC-HA and pCAG-MC-HA, respectively.

**Antibodies.** cDNA encoding the JEV core protein (amino acids 2 to 105) was inserted into pGEX-2TK (Amersham Biosciences, Piscataway, N.J.) and transformed into *Escherichia coli* strain DH5α. The glutathione-*S*-transferase-fused JEV core protein expressed in the bacteria was purified with a column with glutathione Sepharose 4B (Amersham Biosciences) and intradermally injected five times into a Japanese white rabbit purchased from KITAYAMA LABES (Nagano, Japan). The collected antiserum was absorbed with glutathione-*S*-transferase-binding glutathione Sepharose 4B. Anti-JEV monoclonal antibodies (MAb), anti-E 10B4 (E. Konishi, unpublished data) and anti-NS3 34B1 (K. Yasui, unpublished data), were used in immunostaining. Anti-nucleolin MAb, MS-3, and antiactin goat serum were purchased from Santa Cruz Biotechnology (Santa Cruz, Calif.). Rabbit antiserum to PA28 α was purchased from AFFINITI (Exeter, United Kingdom).

**Transfection of plasmids.** Plasmid vectors were transfected by Superfect (QIAGEN, Tokyo, Japan) for Vero cells or Lipofectamine 2000 (Invitrogen, Carlsbad, Calif.) for 293T, BHK, N18, HeLa, HepG2, and SK-N-SH cells. To examine the intracellular localization of the EGFP or EGFP-fused proteins, the cells were fixed with 4% paraformaldehyde in phosphate-buffered saline (PBS) and permeabilized with 0.5% Triton X-100 in PBS at 24 h after transfection. After treatment with 1 μg of RNase A (QIAGEN)/ml, the nuclei were stained with 500 μM propidium iodide (Molecular Probes, Eugene, Oreg.). Endogenous nucleolin, a major nucleolar protein (51), was immunostained by an anti-nucleolin monoclonal antibody and Alexa Flour 564-conjugated anti-mouse immunoglobulin G (IgG) antiserum (Molecular Probes). All samples were visualized with a laser scanning confocal microscope (Bio-Rad, Hercules, Calif.).

**Generation of JEV from plasmid.** The wild-type and mutant (designated M4243) JEVs were generated from plasmids, pMWJEATG1, and pMWJEAT/GP4243AA, respectively, by previous methods (Zhao et al., submitted) with some modifications. Briefly, the plasmid DNAs digested by restriction enzyme KpnI were used as templates for RNA synthesis. Capped full-length JEV RNAs were synthesized in vitro by an mMESSAGE mMACHINE T7 kit (Ambion, Austin, Tex.), purified by precipitation with lithium chloride, and used for electroporation. Trypsinized Vero cells were washed with PBS and resuspended at $10^7$ cells/ml in PBS. RNA (10 μg) was mixed with 500 μl of cell suspension and transferred to an electroporation cuvette (Thermo Hybrid, Middlesex, United Kingdom). Cells were then pulsed at 190 V and 950 μF by the use of a Gene Pulser II apparatus (Bio-Rad). Transfected cells were suspended in a culture medium and transferred to 10-cm-diameter culture dishes. After 3 or 4 days of incubation, the culture supernatants were collected as viral solutions. Due to a low viral yield, these viruses were amplified by a single passage in C6/36 cells. Viral infectivities were determined as focus-forming units (FFUs) by an immunostaining focus assay of Vero, C6/36, and 293T cells. Briefly, viruses were serially diluted and inoculated onto cell monolayers. After 1 h of adsorption, the cells were washed with serum free D-MEM three times and cultured in D-MEM containing 5% FBS and 1.25% methylcellulose 4000. At 2 or 3 days later, the cells were fixed with 4% paraformaldehyde and permeabilized with 0.5% Triton X-100. Infectious foci were stained with an anti-JEV E monoclonal antibody and visualized with a VECTASTAIN Elite ABC anti-mouse IgG kit with a VIP substrate (Vector Laboratories, Burlingame, Calif.). Vero and C6/36 cells infected with wild-type or M4243 JEV were fixed with cold acetone at 48 h postinoculation and stained with the rabbit anti-JEV core protein antiserum and Alexa Flour 488-conjugated goat anti-rabbit IgG (Molecular Probes) antibody. After treatment with 1 μg of RNase A/ml, nuclei were stained with 500 μM propidium iodide. Samples were examined with a laser scanning confocal microscope.

**Subcellular fractionation.** At 48 h postinoculation, $2 \times 10^6$ Vero cells were fractionalized into cytoplasm and nucleus by using a Nuclear/Cytosol Fractionation kit (BioVision, Mountain View, Calif.) according to the manufacturer's instructions. Finally, 210 μl of the cytoplasmic extracts and 100 μl of the nuclear extracts were recovered and 10 μl of each of the extracts was subjected to electrophoresis on an acrylamide gel. The JEV core protein was detected by Western blotting using the anti-JEV core protein rabbit polyclonal antibody. Endogenous PA28α (3, 42) and nucleolin were detected as controls for the cytoplasmic and nuclear fractions, respectively.

**Growth kinetics of mutant JEV in culture cells.** Vero or C6/36 cells ($2 \times 10^5$) in 24-well plates were infected with wild-type or M4243 virus at a multiplicity of infection (MOI) of 5 for 1 h at 4°C, washed three times with a medium to remove unbound viruses, and incubated with a medium supplemented with 5% FBS for a total duration of 30 h. The culture supernatants were used for titration of infectious virus, and cells were used for detection of viral proteins by Western blotting and for detection of negative-strand viral RNA by real-time reverse transcription-PCR (RT-PCR). Total RNAs were extracted from the cells by using an RNeasy Mini kit (QIAGEN) and quantified with a Gene Quant RNA/DNA calculator (Amersham Biosciences). RNA samples (5 μl) were reverse transcribed at 52°C for 30 min with TaqMan reverse transcription reagents (Applied Biosystems, Foster, Calif.) by the use of a negative-strand-specific "tagged" primer corresponding to nucleotides (nt) 9307 to 9332 (5'-GCG TCA TGG TGG CGT ATT TAC CAG AAC TGA TTT AGA AAA TGA A-3'). The tagged sequence, which is underlined, had no correlation to JEV or other flaviviruses. The reverse transcripts were applied to a real-time PCR assay using a TaqMan PCR core reagents kit with sense (5'-GCG TCA TGG TGG CGT

ATT TA-3') and antisense (5'-TGG ACA GCG ATG TTC GTG AA-3') primers corresponding to the tagged sequence and nt 9519 to 9538 of the JEV AT31 strain, respectively. The kinetics of cDNA amplification were monitored with an ABI PRISM 7000 sequence detection system (Applied Biosystems) using a reporter probe corresponding to nt 9363 to 9380 of the JEV AT31 strain (5'-CAC CGC ATG CTC GCC CGA-3') conjugated with 6-carboxyfluorescein at the 5' terminal and 6-carboxy-tetramethylrhodamine at the 3' terminal. As references for the real-time RT-PCR, positive- and negative-strand RNAs were synthesized by in vitro transcription from plasmids containing nt 8907 to 9955 of JEV cDNA inserted in the forward and backward directions under the control of a T7 promoter.

**Characterization of viral particles.** Vero and C6/36 cells were inoculated with wild-type or M4243 viruses at an MOI of 0.1, and culture fluids harvested after 2 (Vero cells) or 3 (C6/36 cells) days postinoculation were clarified by centrifugation at 6,000 × *g* for 30 min and precipitated with 10% polyethylene glycol (molecular mass, approximately 6,000 kDa). The precipitate was collected by centrifugation at 10,000 × *g* for 45 min and resuspended in TN buffer (10 mM Tris-HCl [pH 8.0], 100 mM NaCl). The infectious titers of the concentrated viral particles were determined on Vero cells. The hemagglutination (HA) titers were determined at pH 6.6 by the method of Clarke and Casals (9). The viral particles (400 HA units) were applied on 10 to 40% of sucrose gradients and were centrifuged at 147,000 × *g* for 90 min. Fractions collected from the bottom were examined by the HA test.

**Complementation of mutant virus replication in mammalian cells.** pCAG-WC-HA, pCAG-MC-HA, or pCAG-GS (1 μg) was transfected into 293T cells in a 24-well plate ($5 \times 10^4$ cells). At 4 h after transfection, the cells were washed three times with a serum-free medium and infected with the wild-type or M4243 JEV at an MOI of 5. At 12, 18, and 24 h after inoculation, the culture supernatants were harvested and infectivity was determined on Vero cells. The infected cells were harvested, and expression levels of the core proteins and replication of viral RNA were determined by Western blotting and real-time RT-PCR, respectively.

**Mouse experiments.** Female ICR mice of strain Jcl:ICR (3 weeks old) were purchased from CLEA Japan (Osaka, Japan). All mice were kept in pathogen-free environments. Groups of mice ($n = 10$) were inoculated intracerebrally (ic) with 30 μl of 10-fold-diluted solutions of wild-type or M4243 virus. The virus dilution solution (D-MEM) was administered to 10 mice as a control. The mice were observed for 2 weeks after inoculation to determine survival rates. The value of the 50% lethal dose ($LD_{50}$) for each virus was determined by the method by Reed and Müench (47). Groups of mice ($n = 10$ or 11) were inoculated intraperitoneally (ip) with $10^5$ FFU (100 μl) of the viruses. The mice were observed for 3 weeks after inoculation to determine survival rates. To examine viral growth in the brain, 100 FFU (ic) or $10^5$ FFU (ip) of the viruses were administered to the mice. At 1 to 7 days after inoculation, the mice were euthanized, and the brains were collected. The infectious viral titers in the homogenates of the brains were determined in Vero cells as described above.

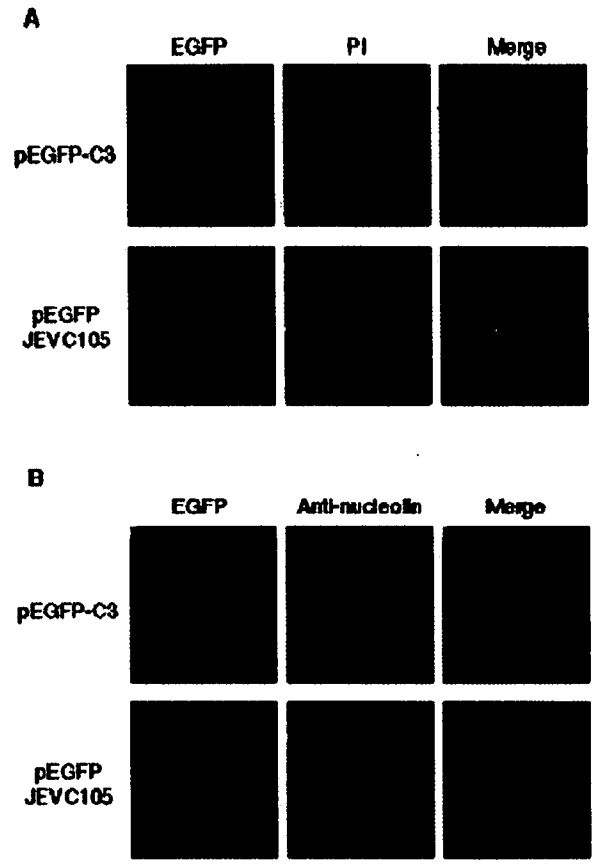


FIG. 1. Intracellular localization of EGFP-fused JEV core protein. Vero cells were transfected with expression plasmids encoding EGFP or EGFP-fused JEV core protein. At 24 h after transfection, cells were fixed with 4% paraformaldehyde and permeabilized with 0.5% Triton X-100. (A) Nuclei were stained with propidium iodide. (B) A representative nucleolar protein, nucleolin, was stained with anti-nucleolin monoclonal antibody. All samples were observed with a confocal microscope.

## RESULTS

**Determination of amino acids essential for nuclear or nucleolar localization of the JEV core protein.** To examine the subcellular localization of the mature JEV core protein without the C-terminal signal sequence in mammalian cells, pEGFP-JEVC105 encoding the EGFP-fused core protein or parental vector, pEGFP-C3, was transfected into Vero cells. EGFP was diffusely distributed in both the cytoplasm and nucleus, while the EGFP-fused core protein exhibited a diffuse distribution in the cytoplasm but granular localization in the nucleus (Fig. 1A). The fusion JEV core protein in the nucleus was colocalized with nucleolin, a major nucleolar component, indicating that the core protein is accumulated at the nucleoli (Fig. 1B). A similar subcellular localization of the fusion core protein was observed in all of the cell lines examined, including neuronal (N18 and SK-N-SH) and nonneuronal (293T, BHK, HeLa, and HepG2) cells (data not shown). Wang et al. (59) reported that the DEN core protein possessed a bipartite NLS in residues 85 to 100 (RKEIGRMLNILNRRKR). A computer program, PSORTII (Institute of Medical Science, Tokyo University [http://psort.ims.u-tokyo.ac.jp/helpwww2.html]), predicted that the JEV core protein also had an NLS at the corresponding region (residues 85 to 101 [KRELGTLIDAVNKRG RK]). To confirm whether the region functions as an NLS, an expression vector for the EGFP-fused mutant core protein in which all of the six basic amino acids (Arg and Lys) that were key amino acids in the NLS motifs were replaced by Ala (AAELGTLIDAVNAAGAA) was transfected into Vero cells. However, these mutations did not affect the nuclear or nucleolar localization of the JEV core protein (data not shown), suggesting that this region of the JEV core protein does not participate as an NLS.

Alternatively, we found another candidate for an NLS in the JEV core protein. The NLS of the core protein of hepatitis C virus (HCV), a member of the same family *Flaviviridae*, has been mapped to the amino acid residues 38 to 43 (54). This domain of the HCV core protein is found to be homologous with flaviviruses, including JEV, St. Louis encephalitis virus, KUN, West Nile virus (WNV), Murray Valley encephalitis virus, and DEN (type 1 to 4) (Fig. 2A). In particular, the two amino acids Gly and Pro are completely conserved among

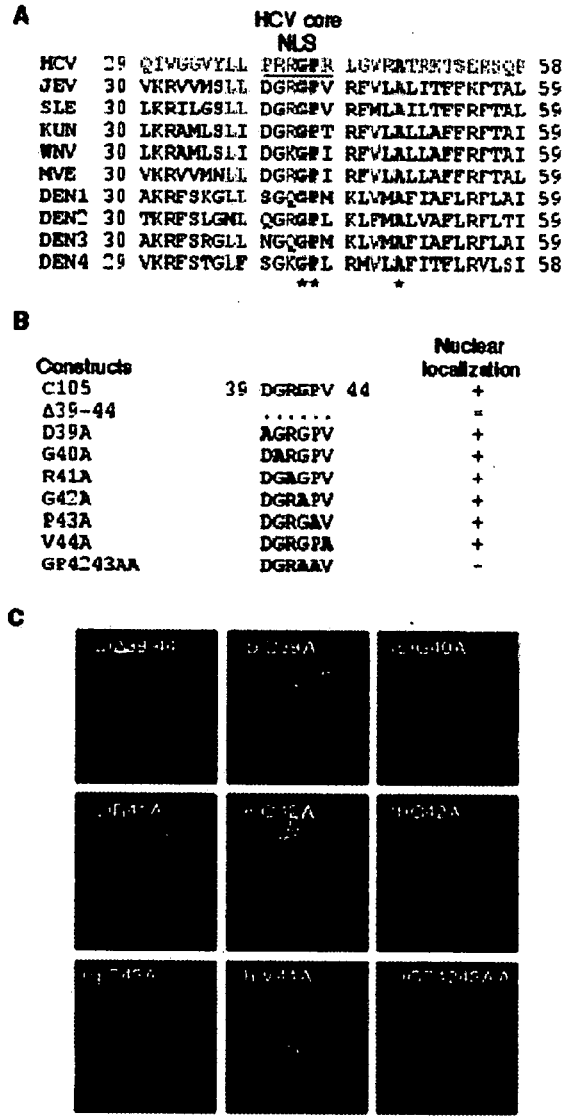


FIG. 2. Role of an HCV core protein NLS in nuclear localization of JEV core protein. (A) A partial alignment of amino acid sequences of core proteins of HCV (HCVJ1 strain, genotype 1b) and flaviviruses, including JEV, SLE (St. Louis encephalitis virus), KUN, WNV, MVE (Murray Valley encephalitis virus), and DENs. Amino acid sequences of the HCV core protein and identical amino acids in flaviviruses are indicated with red letters. Amino acids that were completely conserved among the viruses are indicated by asterisks and red boldface letters. The NLS of HCV core protein previously reported by Suzuki et al. (54) is underlined. (B) Expression plasmids encoding EGFP-fused JEV core proteins mutated in the NLS of the HCV core protein. The presence (+) or absence (−) of nuclear localizations of the EGFP-fused JEV core proteins is indicated. Dots indicate the deleted amino acids. Boldface letters indicate the substituted amino acids. (C) Intracellular localization of EGFP-fused JEV core proteins with deletion or substitution in the NLS region of HCV core protein in Vero cells. Panels (except for panel f) indicate merged images of EGFP and nuclear staining by propidium iodide. Panel f shows merged images of EGFP-fused JEV core protein with a $G^{42}$-to-Ala substitution and a major nucleolar protein nucleolin. All samples were observed with a confocal microscope.

these flaviviruses and HCV. Therefore, we next analyzed the effect of mutation in this region on the nuclear localization of the JEV core protein. The EGFP-fused JEV core protein with residues 39 to 44 deleted was localized only in the cytoplasm but not in the nucleus (Fig. 2B and panel a in Fig. 2C). To further identify the essential amino acids for the nuclear localization, a series of point mutants were constructed (Fig. 2B). No single-amino-acid substitution of the core proteins abolished nuclear localization except for a mutant of $Gly^{42}$ in which the mutant core protein did not colocalize with nucleolin and was distributed as filamentous structures in the nuclei (Fig. 2C, panels e and f). However, double substitutions of the most conserved $Gly^{42}$ and $Pro^{43}$ to Ala completely eliminated the nuclear localization of the JEV core protein (Fig. 2C, panel i). These results indicate that $Gly^{42}$ and $Pro^{43}$, which are well conserved among flaviviruses and HCV (Fig. 2A), are important for nuclear and nucleolar localization of the JEV core protein.

**Mutant JEV lacking the nuclear localization of core protein.** To generate a mutant JEV incapable of localizing the core protein in the nucleus, synthetic RNA transcribed from pMWJEAT/GP4243AA encoding a full-length cDNA of mutant JEV M4243 under the T7 promoter was electroporated into Vero cells. The wild type, which was similarly generated from pMWJEATG1, and M4243 viruses were amplified in C6/36 cells after recovery from Vero cells because of a low viral yield of M4243 virus in Vero cells after electroporation ($2 \times 10^3$ FFU/ml at 3 days after transfection) and used in subsequent experiments. The entire genomic cDNAs of the recovered viruses were confirmed to be identical to those of the infectious clones by direct sequencing. Intracellular localization of core proteins of the wild-type and mutant JEVs was examined in Vero and C6/36 cells by an immunofluorescence assay. In both cell lines, the core protein of the wild-type virus was localized in both the cytoplasm and nuclei whereas the core protein of M4243 was detected only in the cytoplasm and not in nuclei in both cell lines, as we expected (Fig. 3A). To confirm the intracellular localization of the core proteins, cytoplasmic and nuclear fractions of Vero cells infected with the viruses were analyzed by Western blotting (Fig. 3B). The wild-type core protein was fractionated in both cytoplasmic and nuclear fractions, while the mutant core protein was detected in the cytoplasmic fraction but not in the nuclear fraction.

**Growth properties of the mutant JEV in vitro.** To examine the roles of the nuclear localization of the core protein in viral propagation, one-step growth kinetics of the viruses in Vero and C6/36 cells were determined after inoculation at an MOI of 5 (Fig. 4A). The M4243 virus exhibited impaired propagations, with the infectious titers being 773- and 31-fold lower than those of wild-type JEV at 30 h postinoculation in Vero and C6/36 cells, respectively. These results indicate that $Gly^{42}$ and $Pro^{43}$ in the JEV core protein were important for viral propagation, especially in Vero cells. The size of infectious foci in Vero cells produced by the M4243 virus recovered from the culture supernatants at 1 day postinfection of Vero cells was markedly smaller than that of the wild-type virus (Fig. 4B, left and middle panels). However, supernatants of Vero cells recovered 3 days after infection with M4243 produced larger foci than those obtained after incubation for 1 day (Fig. 4B, right panel). This phenomenon was not observed in C6/36 cells. To

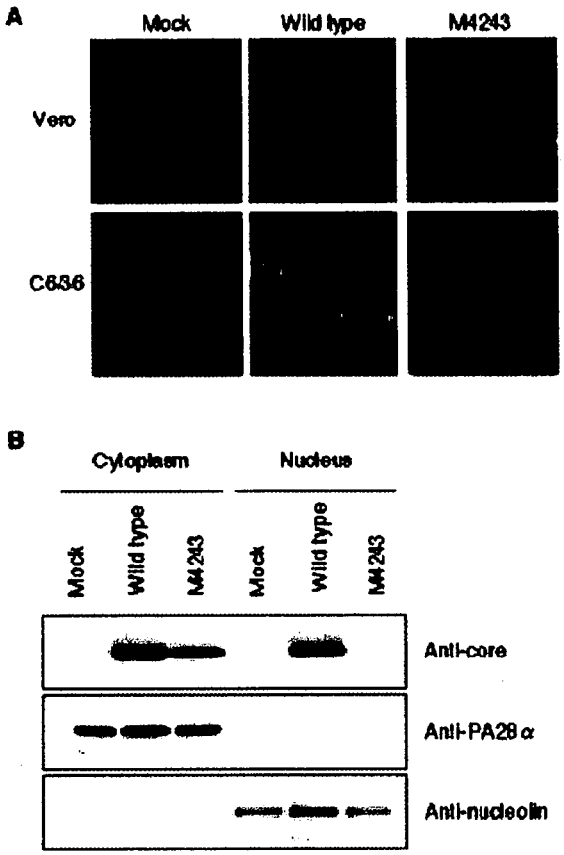


FIG. 3. Intracellular localization of core proteins in cells infected with wild-type or M4243 virus. (A) Intercellular localization of wild-type and mutant JEV. Vero or C6/36 cells were infected with wild-type or M4243 virus, fixed at 2 days postinoculation and immunostained with anti-JEV core rabbit serum. Nuclei were stained with propidium iodide. All samples were observed with a confocal microscope. (B) Intracellular fractionation of Vero cells infected with the viruses. The core proteins in the cytoplasmic and nuclear fractions were detected by Western blotting with the anti-JEV core rabbit serum. Endogenous proteins PA28α and nucleolin were detected as controls for the cytoplasmic and nuclear fractions, respectively.

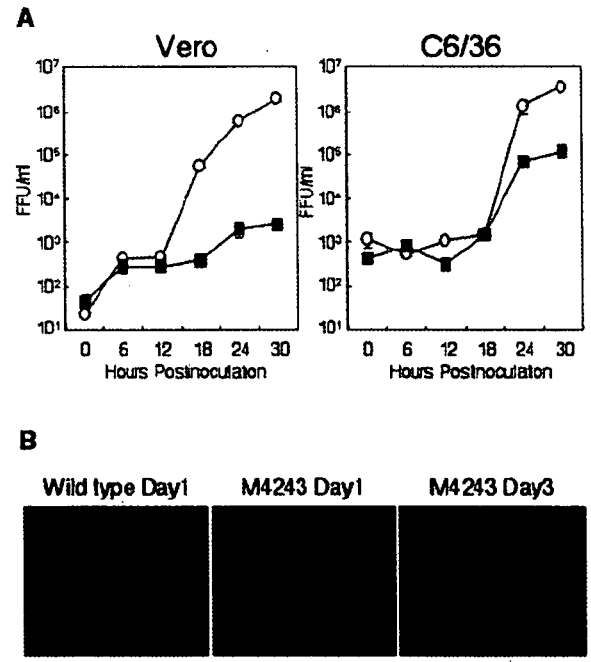


FIG. 4. Growth properties of wild-type and M4243 viruses. (A) Growth kinetics of the viruses in Vero and C6/36 cells. Both cell lines were infected with wild-type or M4243 virus at an MOI of 5. Culture supernatants were harvested at the indicated times postinoculation, and infectious titers were determined by focus-forming assays using Vero cells. Open circles and closed squares indicate the wild-type and M4243 viruses, respectively. Means of three experiments are indicated. (B) Infectious focus formation of the wild-type and M4243 viruses on Vero cells. Culture supernatants recovered at 1 or 3 days postinoculation in Vero cells were inoculated onto Vero cells and incubated for 3 days with methylcellulose overlay medium. The infectious foci were immunostained as described in Materials and Methods.

assess the possibility of the emergence of revertant viruses, the nucleotide sequences of two independent clones obtained at 3 days postinfection with M4243 in Vero cells were determined by direct sequencing. The majority of viruses carried a single-amino-acid reversion from Ala to Gly (GCG to GGG) at residue 42 in both clones. The single mutation of $Pro^{43}$ to Ala of the EGFP-fused JEV core protein did not abolish the nuclear or nucleolar localization, as shown in Fig. 2C (panel g). These results also support the idea that nuclear—especially nucleolar—localization of the JEV core protein is important for viral propagation in Vero cells.

**Characterization of the released particles.** It has been established that the flavivirus core protein is involved in the assembly and budding of infectious particles as a structural protein (34). Mutations in the core protein might posses the possibility to inhibit the release of infectious particles and, inversely, increase production of defective particles as described in previous reports (25, 26). Therefore, we determined the ratios between the infectivities and quantities of the particles released from Vero and C6/36 cells infected with the wild-type or M4243 JEV. The HA assay is able to detect viral particles irrespective of infectivity, because HA activity of the flavivirus is associated with E protein (28, 29). As shown in Table 1, the FFU/HA ratios of the wild-type JEV were significantly higher than those of the M4243 virus in both Vero and C6/36 cells, indicating that the M4243 virus produced a larger amount of defective particles than the wild-type virus. Although the ratios of defective particle production were equivalent between Vero and C6/36 cells, the mutant virus exhibited an HA titer comparable to that of the wild-type virus in C6/36 cells but significantly lower than that of the wild-type virus in Vero cells. In addition, the marked difference of infectious

TABLE 1. Infectious and HA titers of wild type and M4243 viruses derived from Vero and C6/36 cells

| Cell | Virus[a] | FFU/ml | HA/ml | FFU/HA |
|---|---|---|---|---|
| Vero | Wild type | $1.4 \times 10^{10}$ | 25600 | $5.5 \times 10^{5}$ |
| | M4243 | $1.1 \times 10^{6}$ | 400 | $2.8 \times 10^{3}$ |
| C6/36 | Wild type | $1.9 \times 10^{9}$ | 200 | $9.5 \times 10^{6}$ |
| | M4243 | $4.0 \times 10^{7}$ | 800 | $5.0 \times 10^{4}$ |

[a] Viruses were 100-fold concentrated by a polyethylene glycol precipitation and determined the infectivities and HA activities.

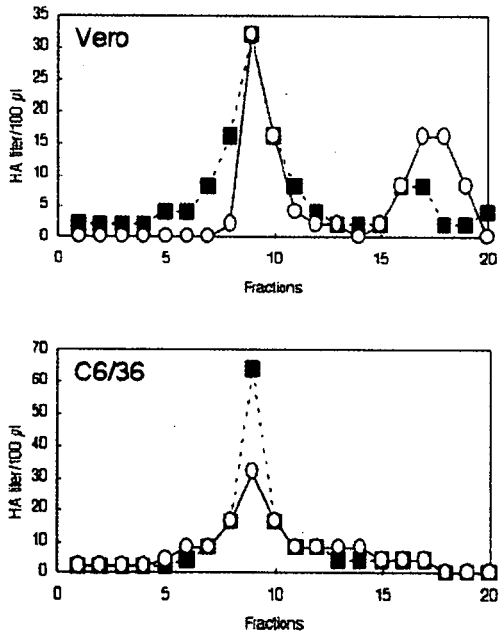


FIG. 5. Gradient fractionation of viral particles of the wild-type and M4243 viruses. The viral particles (400 HA units) derived from Vero or C6/36 cells were applied to 10 to 40% (wt/wt) sucrose gradient and centrifuged at 147,000 × *g* for 90 min. Twenty fractions were collected from bottom to top and quantified by the HA test. Open circles and closed squares indicate the wild-type and M4243 viruses, respectively. The representative data from three experiments are indicated.

titers between the wild-type and M4243 viruses in Vero cells (Fig. 4A) indicates that there may be another mechanism(s) underlying the low-growth properties of the M4243 virus in Vero cells besides the increased production of defective particles. To examine the production of subviral particles in culture supernatants of cells infected with M4243 virus, we carried out gradient fractionations and quantifications of viral particles by HA assay. As indicated in Fig. 5, the patterns of the fractionations of the particles of the M4243 virus were similar to those of the wild-type virus in both Vero and C6/36 cells, and subviral particles were detected in the fractions (fractions 16 to 19) of the supernatants of Vero cells infected with the wild-type or M4243 JEV.

**Effect of nuclear localization of core protein on RNA replication and protein synthesis.** To clarify the reasons for the impaired growth of the M4243 virus in Vero cells, we measured viral RNA replication and protein synthesis in Vero and C6/36 cells infected with wild-type and M4243 viruses. It has been reported that the ratio of the positive strands to the negative strands of viral RNA in JEV-infected cells was 3:1 to 11.7:1 (58). Real-time RT-PCR specific for the negative-strand viral RNA used in this study is capable of detecting more than $10^2$ copies/2 µl of the negative-sense viral RNA in the absence of the positive-strand RNA (Fig. 6A). The amounts of negative-strand RNA in the presence of a 100- or 1,000-fold excess amount of the positive-strand RNA were less than 10-fold different compared with those determined in the absence of the positive-strand RNA (Fig. 6A), indicating that the PCR system is specific enough to measure the negative-strand viral RNA levels in cells infected with JEV. We then measured the synthesis of the negative-strand viral RNAs in Vero and C6/36 cells infected with wild-type or mutant JEV at an MOI of 5 by RT-PCR. Although similar levels of negative-strand RNA synthesis were observed in C6/36 cells infected with either virus, M4243 exhibited 3- and 18-fold-lower RNA replication than the wild type in Vero cells at 18 and 30 h postinoculation, respectively (Fig. 6B). Metabolic labeling of the host proteins indicated that there were no significant differences between the viabilities of Vero cells infected with wild-type and M4243 virus (data not shown). To determine the level of impairment of RNA translation of M4243 in Vero cells, viral protein syn-

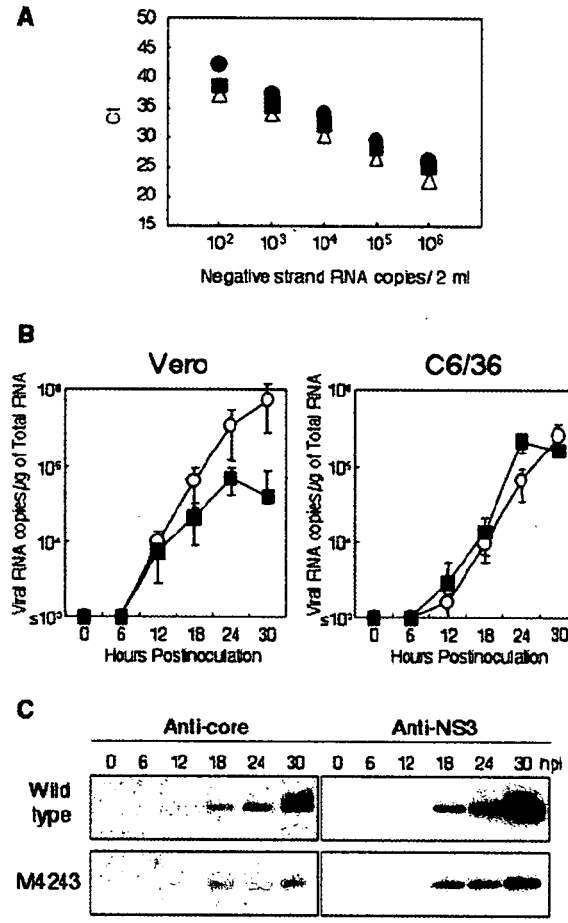


FIG. 6. Viral RNA and protein syntheses in Vero and C6/36 cells infected with wild-type or M4243 virus. (A) Establishment of negative-strand JEV RNA-specific real-time RT-PCR. A series of 10-fold dilutions of synthetic negative-strand RNA in the absence (closed circles) or presence of 100-fold (gray squares) or 1,000-fold (open triangles) synthetic positive-strand RNAs were applied to the real-time RT-PCR. The Ct value represents the first PCR cycle to detect the increase in signal associated with an exponential growth of PCR product. (B) Viral negative-strand RNAs were quantified in the infected cells by the real-time RT-PCR. Open circles and closed squares indicate wild-type and M4243 viruses, respectively. The detection limit was $10^3$ copies of viral RNA/µg of total RNA. Means of three experiments are indicated. (C) Core and NS3 proteins were detected by Western blotting with anti-JEV core rabbit serum and anti-JEV NS3 MAb 34A1, respectively. A total of 4 µg of each sample was loaded.

theses in Vero cells infected with the wild-type or M4243 virus were analyzed by Western blotting (Fig. 6C). Although comparable amounts of core and NS3 proteins were detected at an early phase of infection (12 and 18 h postinoculation) in Vero cells infected with either virus, saturation of protein syntheses by a mutant virus was observed at 24 h postinfection, in contrast to cells infected with the wild-type virus, in which protein synthesis increased until 30 h postinfection. The early saturation of viral protein synthesis of M4243 in Vero cells is quite consistent with that of RNA replication. These results suggest that nuclear localization of the core protein plays a crucial role in the maintenance of replication-translation of viral RNA in mammalian cells but not in mosquito cells, in which the mutant virus replicates at a rate similar to that of the wild-type JEV.

**Complementation of mutant virus replication by expression of the wild-type core protein.** We next examined the growth of a mutant virus in cells transiently expressing the wild-type or mutant core protein. The efficiency of gene transduction into Vero cells is very low, and we therefore selected 293T cells for their high efficiency of foreign-gene transduction and used them to transiently express the JEV core protein. HA-tagged wild-type and mutant core proteins (approximately 16 kDa) and the viral core protein derived from M4243 (approximately 14 kDa) were detected in 293T cells transfected with the expression plasmids and infected with M4243 virus (Fig. 7A). Expression of the wild-type core protein, but not that of the mutant core protein, drastically enhanced viral growth of the M4243 virus up to the level of wild-type virus growth (Fig. 7B). However, the expression of the core proteins did not affect the replication of the wild-type virus. Furthermore, the negative-strand RNA synthesis of the mutant virus was increased threefold by the expression of the wild-type core protein, but not by that of the mutant protein, compared with mock-transfection results (Fig. 7C). These results indicate that the expression of the wild-type JEV core protein is able to compensate for the propagation of the M4243 virus.

**Neurovirulence and neuroinvasiveness of M4243.** To examine the neurovirulence characteristics of the wild-type and mutant viruses, we determined the $LD_{50}$ values by intracerebral inoculation of the viruses into 3-week-old ICR mice. The $LD_{50}$ values for the wild-type and the mutant viruses were 2.1 and 0.5 FFU, respectively. No significant differences in symptoms, mean duration period of diseases (wild versus mutant, 1.1 versus 0.9 days), and mean day of death (7.5 versus 7.6 days postinoculation) were observed between mice inoculated with 100 FFU of the wild-type virus and those inoculated with an equivalent dose of M4243 virus. To examine the growth kinetics of the viruses in the brain, 100 FFU of each virus was intracerebrally injected, and the viruses recovered from the brain homogenates were titrated. The growth of the M4243 virus was approximately 100 times lower than that of the wild-type virus (Fig. 8A, left panel), and revertant viruses exhibiting medium-sized plaques (Fig. 4B) were not recovered from the brains inoculated with the M4243 virus. The neuroinvasiveness of encephalitis flaviviruses is thought to be a reflection of their ability to grow in the peripheral organs, to breach the blood-brain barrier, and to infect central nervous systems following peripheral inoculation. To examine the neuroinvasiveness of wild-type and M4243 viruses, ICR mice were intraperitoneally

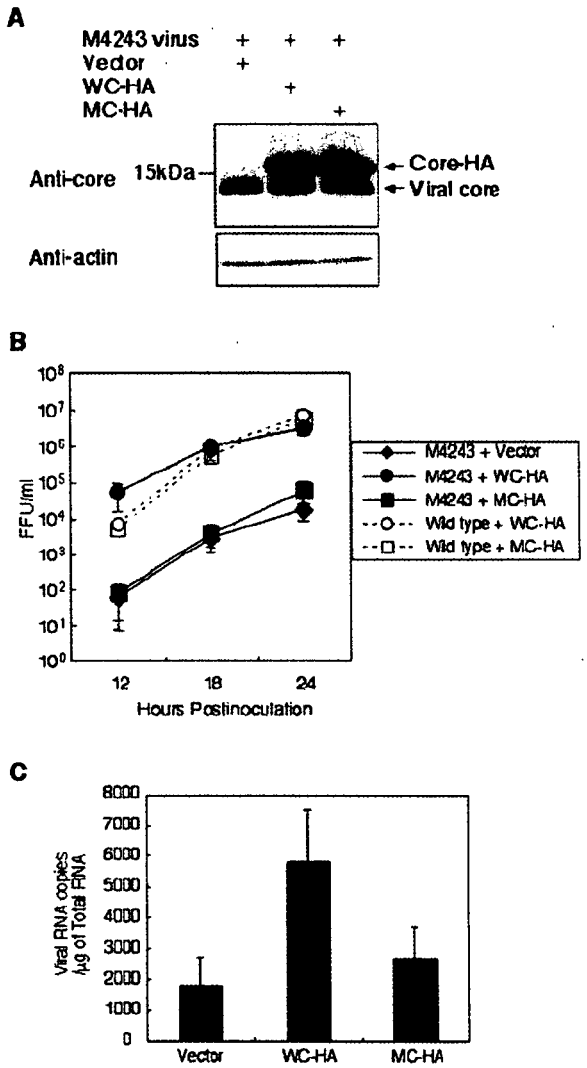


FIG. 7. Complementation of M4243 replication by expression of core proteins in 293T cells. At 4 h after transfection with pCAG-GS (Vector), pCAG-WC-HA (WC-HA), or pCAG-MC-HA ($Gly^{42}$ and $Pro^{43}$ to Ala) (MC-HA), 293T cells were infected with wild-type or M4243 virus at an MOI of 5. At 12, 18, or 24 h postinoculation, culture supernatants and cells were harvested to apply to focus-forming assays and Western blotting or real-time RT-PCR, respectively. (A) Western blotting of 293T cells transfected with plasmids expressing HA-tagged wild-type or mutant core protein and infected with M4243 virus. Molecular mass marker was indicated in the left of the panel. (B) Growth of wild-type and M4243 viruses in 293T cells transfected with the plasmids. Viral titers were determined by focus-forming assays in Vero cells. (C) Complementation of M4243 in 293T cells transfected with the plasmids at 24 h postinoculation. Viral RNA levels were determined by the negative-strand-specific real-time RT-PCR. Means from three experiments are indicated.

inoculated with $10^5$ FFU of each virus. Only 1 of 11 mice inoculated with the M4243 virus had died by 9 days postinoculation, while on average 10 of the 11 mice inoculated with the wild-type virus had died by 9.6 days postinoculation (Fig. 8B). Over 5 days after inoculation, the viruses were recovered from the brain of mice inoculated with wild-type JEV but not from those inoculated with M4243 (Fig. 8A, right panel). These re-

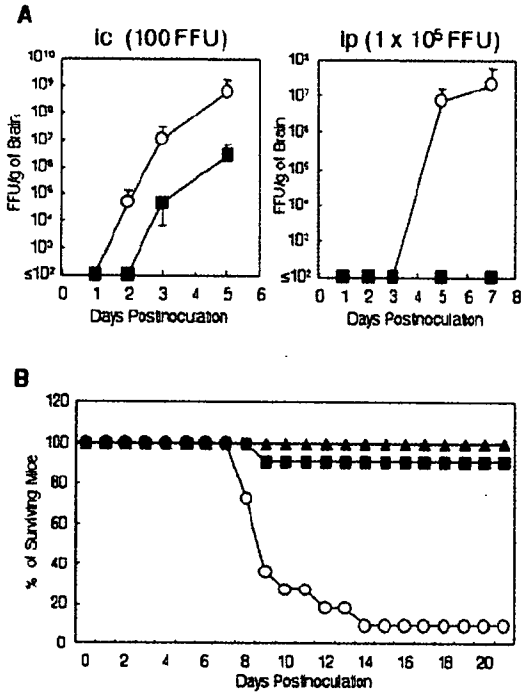


FIG. 8. Virulence of wild-type and M4243 viruses for ICR mice. (A) The infectious titers of wild-type and M4243 viruses in the brains of mice after inoculation with 100 FFU of the viruses intracerebrally (ic) or $10^5$ FFU intraperitoneally (ip). Open circles and closed squares indicate wild-type and M4243 viruses, respectively. The detection limit is $10^2$ FFU/gram of brain. Means of titers from four mice are indicated. (B) Percentages of surviving mice (10 to 11 mice per group) inoculated with $10^5$ FFU of wild-type or M4243 viruses by an intraperitoneal route. Open circles, closed squares, and gray triangles indicate mice infected with the wild-type virus, infected with the M4243 virus, or mock infected, respectively.

sults indicated that the mutant virus exhibited a level of neurovirulence equivalent to that of the wild type but that its neuroinvasiveness was severely impaired in 3-week-old-ICR mice.

## DISCUSSION

Like most animal RNA viruses, except for those of the families *Orthomyxoviridae*, *Bornaviridae*, and *Retroviridae*, members of the *Flaviviridae* replicate in the cytoplasm of host cells (34). However, it has been reported that the core proteins of DEN, KUN, and HCV are observed not only in the cytoplasm but also in the nucleus (4, 38, 55, 59, 61). In this study, we demonstrated that the JEV core protein was translocated into the nucleus and accumulated in the nucleolus of cells infected with JEV or transfected with an expression plasmid for the core protein. We revealed that $Gly^{42}$ and $Pro^{43}$ were important for the nuclear localization and that $Gly^{42}$ was essential for the nucleolar accumulation of the JEV core protein. The two amino acids Gly and Pro are well conserved not only among mosquitoborne flaviviruses such as JEV, KUN, WNV, and DEN but also among HCVs. According to the three-dimensional structures of KUN and DEN, the two amino acids are mapped to the unsheltered loop domain between α-helices 1 and 2 (11, 36). Substitutions of $Gly^{42}$ and $Pro^{43}$ with Ala completely abolished the nuclear localization of the JEV core protein as well as that of the DEN core protein (data not shown). However, a previous study showed that deletion of the N-terminal 45 amino acids of the DEN core protein did not eliminate nuclear localization of the protein (59). Although the reason for this discrepancy is not presently clear, our data suggest that the well-conserved Gly and Pro are important for nuclear or nucleolar localization of the core protein of flaviviruses. The two amino acids and the flanking sequences exhibited no similarity to the well-known classical NLSs, such as a large T-antigen of simian virus 40 (PKKKRKV) (21), nucleoplasmin (KRPAATKKAGQAKKKK) (5), and nucleolar localization signals, such as the Rex protein of human T-cell leukemia virus type I (MPKTRRRPRRSQRKRPPTP) (44). This domain may be required for recognition of novel nuclear import receptor protein(s) and nucleolar component(s). Recently, Dokland et al. demonstrated that tetramers of the KUN core protein extended as filamentous ribbon structures (11). The change of $Gly^{42}$ to Ala in the JEV core protein, therefore, may abolish the binding activity to nucleolar compartment(s) and exhibit a filamentous structure in the nuclei (Fig. 2C).

The recovery of the M4243 virus in which Ala was substituted for $Gly^{42}$ and $Pro^{43}$ of the core protein suggests that nuclear localization of the core protein is not a necessary condition for viral propagation. However, replication of the mutant virus was impaired in mammalian cells but not in mosquito cells. The impairment of propagation of the M4243 virus in mammalian cells may be due to either of two phenomena: the decrease in production of infectious particles with a simultaneous increase of defective particles or the low efficiency of viral RNA replication. Since budding of flavivirus takes place through the interaction of prM and E proteins independently of the association with the core protein, disfunctions of core protein may reduce the production of infectious particles and enhance the production of subviral particles. In fact, mutations at the cleavage site of host signal peptidase in the core-prM junction of Murray Valley encephalitis virus caused an increase of subviral particle production (35). Furthermore, TBEV core proteins with deletions of the central hydrophobic region, containing $Gly^{36}$ corresponding to the $Gly^{42}$ essential for nucleolar localization of the JEV core protein, increased the production of subviral particles due to the lack of association with the ER membrane, where budding of the flavivirus takes place (26, 27). In contrast, the mutations on the $Gly^{42}$ and $Pro^{43}$ region of the JEV core protein caused the production of the defective particles different from subviral particles. Although the mechanisms underlying the production of the defective particles remain unclear, the mutations might affect the functions except for assembly and budding, such as maturation or uncoating. As far as we know, biological functions except for nuclear localization in the $Gly^{42}$ and $Pro^{43}$ region of the flavivirus core proteins have not been studied. The mutations might collaterally disrupt the conformation of the core protein essential for their functions of JEV. Meanwhile, it might be feasible that the nuclear localization of the core protein directly participates in the viral infectivity. Tijms et al. (56) demonstrated that the capsid protein of equine arteritis virus mostly shuffled between the cytoplasm and nucleus prior to cytoplasmic viral assembly, suggesting that the nuclear localization is crucial for viral assembly. In any case, production of the defective particles by the mutant JEV was enhanced in both Vero and C6/36 cells, and

thus, a decrease of infectious particles cannot explain the impairment of M4243 in Vero cells.

It is believed that the core protein is not required for RNA replication, since the RNA replicon of flavivirus, which does not contain the whole core gene, has been shown to be capable of replicating (10, 13, 24). Therefore, it is noteworthy that RNA replication of M4243 was impaired in Vero cells but not in mosquito cells. Although a *cis*-acting nucleotide sequence element essential for RNA replication has been mapped to the flavivirus core genes (10, 22), the nucleotide changes were not involved in the impairment of replication of M4243 due to the compensation of RNA replication by the expression of wild-type core protein in *trans*. The kinetics study of viral RNA and protein syntheses suggested that the JEV core protein translated at the early step of infection was translocated into the nucleus and enhanced RNA replication at the late phase of infection, although further studies are needed to clarify the precise mechanism. Earlier studies (30, 31) resulted in reports that flaviviruses, including JEV, but not alphaviruses failed to propagate and produce viral antigens in cells enucleated by cytochalasin B, suggesting the involvement of host nucleus factors in flavivirus replication. The DEN core protein was reported to interact with a nuclear transcription factor, heterogeneous nuclear ribonucleoprotein K, and regulate the C/EBP-β-mediated transcription (7). Furthermore, the HCV core protein was also shown to associate with host nuclear proteins such as heterogeneous nuclear ribonucleoprotein K (18) and PA28γ (42) and was suggested to regulate the transcription of host cells (18, 45). The nuclear localization of core proteins of *Flaviviridae* might change the suitability of the host-cell environment for viral propagation by producing factors that enhance RNA replication or by suppressing those that reduce it.

Other cytoplasmic RNA viruses, such as members of the families *Picornaviridae* (1, 2, 12), *Coronaviridae* (8, 15, 62), *Arteriviridae* (48, 56), *Togaviridae* (41), and *Rhabdoviridae* (46), may also feed their proteins into the nucleus to facilitate viral propagation. For example, it is suggested that the protein 2A of encephalomyocarditis virus is localized to the nucleoli and inhibits cellular mRNA transcription (1) and that point mutations within the NLS of another nucleolar protein, $3D^{Pol}$, were lethal due to the inhibition of viral RNA replication (2). The coronavirus nucleoproteins were also found to be localized in the nucleoli of the host cells (8, 15, 62), and the expression of the coronavirus nucleoproteins by transfection inhibits host cell division (8, 62).

Surprisingly, the M4243 virus exhibited a high level of neurovirulence in mice comparable to that of the wild-type JEV despite the fact that the M4243 virus had a 100-fold-lower replication efficiency than the wild-type JEV in vivo. Encephalitis induced by flavivirus infection is thought to arise from direct injury of brain neurons by viral replication (49, 64) or indirect injury of brain neurons by immune responses (60). However, the idea that the direct injury of neurons is responsible for encephalitis induced by flavivirus is difficult to reconcile with the results showing that the virulence of the M4243 virus is equivalent to that of the wild-type virus. A previous study indicated that a low dose of WNV-induced encephalitis was associated with inflammatory cell infiltration in mice (60). Alternatively, the defective particles contained in the inoculum or produced by M4243 infections might stimulate a signal pathway via reactive oxygen species in neuronal cells and induce cell death, as described by Lin et al. (33).

In contrast to the neurovirulence results, a striking difference in levels of neuroinvasiveness was observed between the wild-type and M4243 viruses. Although the magnitude and duration of viremia were suggested to be major determinants for neuroinvasion (19, 32), the precise mechanism by which flaviviruses breach the blood-brain barrier and enter the brain tissue remains uncertain. Encephalitis flaviviruses injected by peripheral routes are thought to replicate in lymphatic tissues, such as peripheral lymph nodes or spleen, and to induce further viremia (32, 40). Although we had no evidence that JEV replicated in peripheral tissues prior to neuroinvasion as described by others (32), the wild-type virus, but not M4243, was present in small amounts (100 to 200 FFU/ml) in blood samples at 1 and 3 days postinoculation (data not shown). In this context, it might be possible that the M4243 virus was unable to replicate in peripheral tissues at a level sufficient to develop viremia and breach the blood-brain barrier, resulting in the low level of neuroinvasiveness. The novel attenuation of neuroinvasiveness observed in M4243 may be applicable to the development of new live vaccines against flavivirus infection.

The life cycles of most flaviviruses are sustained between arthropods and vertebrates. The present finding that nuclear localization of the core protein enhances viral replication in mammalian cells may lead to an improved understanding of the evolutionary adaptation strategy of flaviviruses in expanding their host range from arthropods to vertebrates. It might also be possible to speculate that JEV transgressed its host barrier by translocating the core protein into the nucleus of porcine cells and incorporated the pig as an amplifier in the life cycle of JEV. Furthermore, it is of interest for evolutional studies on the family *Flaviviridae* that the NLSs of core proteins were well conserved between mosquitoborne flaviviruses and bloodborne and human-adapted HCV.

## ACKNOWLEDGMENTS

We thank T. Shioda, Osaka University, for advice on the confocal microscopy. We also thank H. Murase and I. Yanase for secretarial work.

This work was supported in part by grants-in-aid from the Ministry of Health, Labor and Welfare, the program for Promotion of Fundamental Studies in Health Sciences of the Organization for Drug ADR Relief, R&D Promotion, and Product Review, the Ministry of Education, Culture, Sports, Science and Technology, and the 21st Century Center of Excellence Program of Japan.

## REFERENCES

1. **Aminev, A. G., S. P. Amineva, and A. C. Palmenberg.** 2003. Encephalomyocarditis viral protein 2A localizes to nucleoli and inhibits cap-dependent mRNA translation. Virus Res. 95:45–57.
2. **Aminev, A. G., S. P. Amineva, and A. C. Palmenberg.** 2003. Encephalomyocarditis virus (EMCV) proteins 2A and 3BCD localize to nuclei and inhibit cellular mRNA transcription but not rRNA transcription. Virus Res. 95: 59–73.
3. **Brooks, P., G. Fuertes, R. Z. Murray, S. Bose, E. Knecht, M. C. Rechsteiner, K. B. Hendil, K. Tanaka, J. Dyson, and J. Rivett.** 2000. Subcellular localization of proteasomes and their regulatory complexes in mammalian cells. Biochem. J. 346:155–161.
4. **Bulich, R., and J. G. Aaskov.** 1992. Nuclear localization of dengue 2 virus core protein detected with monoclonal antibodies. J. Gen. Virol. 73:2999–3003.
5. **Bürglin, T. R., and E. M. De Robertis.** 1987. The nuclear migration signal of *Xenopus laevis* nucleoplasmin. EMBO J. 6:2617–2625.
6. **Burke, D. S., and T. P. Monath.** 2001. Flaviviruses, p. 1043–1125. *In* D. M. Knipe, P. M. Howley, D. E. Griffin, R. A. Lamb, M. A. Martin, B. Roizman,

and S. E. Straus (ed.), Fields virology, 4th ed., vol. 1. Lippincott Williams & Wilkins, Philadelphia, Pa.
7. Chang, C. J., H. W. Luh, S. H. Wang, H. J. Lin, S. C. Lee, and S. T. Hu. 2001. The heterogeneous nuclear ribonucleoprotein K (hnRNP K) interacts with dengue virus core protein. DNA Cell Biol. 20:569–577.
8. Chen, H., T. Wurm, P. Britton, G. Brooks, and J. A. Hiscox. 2002. Interaction of the coronavirus nucleoprotein with nucleolar antigens and the host cell. J. Virol. 76:5233–5250.
9. Clarke, D. H., and J. Casals. 1958. Techniques for hemagglutination and hemagglutination-inhibition with arthropod-borne viruses. Am. J. Trop. Med. Hyg. 7:561–573.
10. Corver, J., E. Lenches, K. Smith, R. A. Robison, T. Sando, E. G. Strauss, and J. H. Strauss. 2003. Fine mapping of a *cis*-acting sequence element in yellow fever virus RNA that is required for RNA replication and cyclization. J. Virol. 77:2265–2270.
11. Dokland, T., M. Walsh, J. M. Mackenzie, A. A. Khromykh, K. H. Ee, and S. Wang. 2004. West Nile virus core protein; tetramer structure and ribbon formation. Structure 12:1157–1163.
12. Fernandez-Tomas, C. 1982. The presence of viral-induced proteins in nuclei from poliovirus-infected HeLa cells. Virology 116:629–634.
13. Gehrke, R., M. Ecker, S. W. Aberle, S. L. Allison, F. X. Heinz, and C. W. Mandl. 2003. Incorporation of tick-borne encephalitis virus replicons into virus-like particles by a packaging cell line. J. Virol. 77:8924–8933.
14. Higuchi, R., B. Krummel, and R. K. Saiki. 1988. A general method of in vitro preparation and specific mutagenesis of DNA fragments: study of protein and DNA interactions. Nucleic Acids Res. 16:7351–7367.
15. Hiscox, J. A., T. Wurm, L. Wilson, P. Britton, D. Cavanagh, and G. Brooks. 2001. The coronavirus infectious bronchitis virus nucleoprotein localizes to the nucleolus. J. Virol. 75:506–512.
16. Ho, S. N., H. D. Hunt, R. M. Horton, J. K. Pullen, and L. R. Pease. 1989. Site-directed mutagenesis by overlap extension using the polymerase chain reaction. Gene 77:51–59.
17. Horton, R. M., H. D. Hunt, S. N. Ho, J. K. Pullen, and L. R. Pease. 1989. Engineering hybrid genes without the use of restriction enzymes: gene splicing by overlap extension. Gene 77:61–68.
18. Hsieh, T. Y., M. Matsumoto, H. C. Chou, R. Schneider, S. B. Hwang, A. S. Lee, and M. M. Lai. 1998. Hepatitis C virus core protein interacts with heterogeneous nuclear ribonucleoprotein K. J. Biol. Chem. 273:17651–17659.
19. Huang, C. H., and C. Wong. 1963. Relation of the peripheral multiplication of Japanese B encephalitis virus to the pathogenesis of the infection in mice. Acta Virol. 7:322–330.
20. Jones, C. T., L. Ma, J. W. Burgner, T. D. Groesch, C. B. Post, and R. J. Kuhn. 2003. Flavivirus capsid is a dimeric alpha-helical protein. J. Virol. 77:7143–7149.
21. Kalderon, D., W. D. Richardson, A. F. Markham, and A. E. Smith. 1984. Sequence requirements for nuclear location of simian virus 40 large-T antigen. Nature 311:33–38.
22. Khromykh, A. A., H. Meka, K. J. Guyatt, and E. G. Westaway. 2001. Essential role of cyclization sequences in flavivirus RNA replication. J. Virol. 75:6719–6728.
23. Khromykh, A. A., and E. G. Westaway. 1996. RNA binding properties of core protein of the flavivirus Kunjin. Arch. Virol. 141:685–699.
24. Khromykh, A. A., and E. G. Westaway. 1997. Subgenomic replicons of the flavivirus Kunjin: construction and applications. J. Virol. 71:1497–1505.
25. Kofler, R. M., J. H. Aberle, S. W. Aberle, S. L. Allison, F. X. Heinz, and C. W. Mandl. 2004. Mimicking live flavivirus immunization with a noninfectious RNA vaccine. Proc. Natl. Acad. Sci. USA 101:1951–1956.
26. Kofler, R. M., F. X. Heinz, and C. W. Mandl. 2002. Capsid protein C of tick-borne encephalitis virus tolerates large internal deletions and is a favorable target for attenuation of virulence. J. Virol. 76:3534–3543.
27. Kofler, R. M., A. Leitner, G. O'Riordain, F. X. Heinz, and C. W. Mandl. 2003. Spontaneous mutations restore the viability of tick-borne encephalitis virus mutants with large deletions in protein C. J. Virol. 77:443–451.
28. Konishi, E., S. Pincus, B. A. Fonseca, R. E. Shope, E. Paoletti, and P. W. Mason. 1991. Comparison of protective immunity elicited by recombinant vaccinia viruses that synthesize E or NS1 of Japanese encephalitis virus. Virology 185:401–410.
29. Konishi, E., S. Pincus, E. Paoletti, R. E. Shope, T. Burrage, and P. W. Mason. 1992. Mice immunized with a subviral particle containing the Japanese encephalitis virus prM/M and E proteins are protected from lethal JEV infection. Virology 188:714–720.
30. Kos, K. A., B. A. Osborne, and R. A. Goldsby. 1975. Inhibition of group B arbovirus antigen production and replication in cells enucleated with cytochalasin B. J. Virol. 15:913–917.
31. Lad, V. J., A. K. Gupta, S. N. Ghosh, and K. Banerjee. 1993. Immunofluorescence studies on the replication of some arboviruses in nucleated and enucleated cells. Acta Virol. 37:79–83.
32. Lee, E., and M. Lobigs. 2002. Mechanism of virulence attenuation of glycosaminoglycan-binding variants of Japanese encephalitis virus and Murray Valley encephalitis virus. J. Virol. 76:4901–4911.
33. Lin, R. J., C. L. Liao, and Y. L. Lin. 2004. Replication-incompetent virions of Japanese encephalitis virus trigger neuronal cell death by oxidative stress in a culture system. J. Gen. Virol. 85:521–533.
34. Lindenbach, B. D., and C. M. Rice. 2001. *Flaviviridae*: The viruses and their replication, p. 991–1041. *In* D. M. Knipe, P. M. Howley, D. E. Griffin, R. A. Lamb, M. A. Martin, B. Roizman, and S. E. Straus (ed.). Fields virology, 4th ed., vol. 1. Lippincott Williams & Wilkins, Philadelphia, Pa.
35. Lobigs, M., and E. Lee. 2004. Inefficient signalase cleavage promotes efficient nucleocapsid incorporation into budding flavivirus membranes. J. Virol. 78:178–186.
36. Ma, L., C. T. Jones, T. D. Groesch, R. J. Kuhn, and C. B. Post. 2004. Solution structure of dengue virus capsid protein reveals another fold. Proc. Natl. Acad. Sci. USA 101:3414–3419.
37. Macara, I. G. 2001. Transport into and out of the nucleus. Microbiol. Mol. Biol. Rev. 65:570–594.
38. Makino, Y., M. Tadano, T. Anzai, S. P. Ma, S. Yasuda, and T. Fukunaga. 1989. Detection of dengue 4 virus core protein in the nucleus. II. Antibody against dengue 4 core protein produced by a recombinant baculovirus reacts with the antigen in the nucleus. J. Gen. Virol. 70:1417–1425.
39. Markoff, L., B. Falgout, and A. Chang. 1997. A conserved internal hydrophobic domain mediates the stable membrane integration of the dengue virus capsid protein. Virology 233:105–117.
40. McMinn, P. C., L. Dalgarno, and R. C. Weir. 1996. A comparison of the spread of Murray Valley encephalitis viruses of high or low neuroinvasiveness in the tissues of Swiss mice after peripheral inoculation. Virology 220:414–423.
41. Michel, M. R., M. Elgizoli, Y. Dai, R. Jakob, H. Koblet, and A.-P. Arrigo. 1990. Karyophilic properties of Semliki Forest virus nucleocapsid protein. J. Virol. 64:5123–5131.
42. Moriishi, K., T. Okabayashi, K. Nakai, K. Moriya, K. Koike, S. Murata, T. Chiba, K. Tanaka, R. Suzuki, T. Suzuki, T. Miyamura, and Y. Matsuura. 2003. Proteasome activator PA28γ-dependent nuclear retention and degradation of hepatitis C virus core protein. J. Virol. 77:10237–10249.
43. Niwa, H., K. Yamamura, and J. Miyazaki. 1991. Efficient selection for high-expression transfectants with a novel eukaryotic vector. Gene 108:193–199.
44. Nosaka, T., H. Siomi, Y. Adachi, M. Ishibashi, S. Kubota, M. Maki, and M. Hatanaka. 1989. Nucleolar targeting signal of human T-cell leukemia virus type I rex-encoded protein is essential for cytoplasmic accumulation of unspliced viral mRNA. Proc. Natl. Acad. Sci. USA 86:9798–9802.
45. Otsuka, M., N. Kato, K. Lan, H. Yoshida, J. Kato, T. Goto, Y. Shiratori, and M. Omata. 2000. Hepatitis C virus core protein enhances p53 function through augmentation of DNA binding affinity and transcriptional ability. J. Biol. Chem. 275:34122–34130.
46. Petersen, J. M., L. S. Her, V. Varvel, E. Lund, and J. E. Dahlberg. 2000. The matrix protein of vesicular stomatitis virus inhibits nucleocytoplasmic transport when it is in the nucleus and associated with nuclear pore complexes. Mol. Cell. Biol. 20:8590–8601.
47. Reed, L. J., and H. Müench. 1938. A simple method of estimating fifty per cent endpoints. Am. J. Hyg. 27:493.
48. Rowland, R. R., R. Kervin, C. Kuckleburg, A. Sperlich, and D. A. Benfield. 1999. The localization of porcine reproductive and respiratory syndrome virus nucleocapsid protein to the nucleolus of infected cells and identification of a potential nucleolar localization signal sequence. Virus Res. 64:1–12.
49. Shrestha, B., D. Gottlieb, and M. S. Diamond. 2003. Infection and injury of neurons by West Nile encephalitis virus. J. Virol. 77:13203–13213.
50. Solomon, T., H. Ni, D. W. Beasley, M. Ekkelenkamp, M. J. Cardosa, and A. D. Barrett. 2003. Origin and evolution of Japanese encephalitis virus in southeast Asia. J. Virol. 77:3091–3098.
51. Spector, D. L., R. L. Ochs, and H. Busch. 1984. Silver staining, immunofluorescence, and immunoelectron microscopic localization of nucleolar phosphoproteins B23 and C23. Chromosoma 90:139–148.
52. Stocks, C. E., and M. Lobigs. 1998. Signal peptidase cleavage at the flavivirus C-prM junction: dependence on the viral NS2B-3 protease for efficient processing requires determinants in C, the signal peptide, and prM. J. Virol. 72:2141–2149.
53. Sumiyoshi, H., C. Mori, I. Fuke, K. Morita, S. Kuhara, J. Kondou, Y. Kikuchi, H. Nagamatu, and A. Igarashi. 1987. Complete nucleotide sequence of the Japanese encephalitis virus genome RNA. Virology 161:497–510.
54. Suzuki, R., Y. Matsuura, T. Suzuki, A. Ando, J. Chiba, S. Harada, I. Saito, and T. Miyamura. 1995. Nuclear localization of the truncated hepatitis C virus core protein with its hydrophobic C terminus deleted. J. Gen. Virol. 76:53–61.
55. Tadano, M., Y. Makino, T. Fukunaga, Y. Okuno, and K. Fukai. 1989. Detection of dengue 4 virus core protein in the nucleus. I. A monoclonal antibody to dengue 4 virus reacts with the antigen in the nucleus and cytoplasm. J. Gen. Virol. 70:1409–1415.
56. Tijms, M. A., Y. van der Meer, and E. J. Snijder. 2002. Nuclear localization of non-structural protein 1 and nucleocapsid protein of equine arteritis virus. J. Gen. Virol. 83:795–800.
57. Tsai, T. F. 2000. New initiatives for the control of Japanese encephalitis by vaccination: minutes of a W.H.O./CVI meeting, Bangkok, Thailand, 13–15 October 1998. Vaccine 18:1–25.
58. Uchil, P. D., and V. Satchidanandam. 2003. Architecture of the flaviviral replication complex. Protease, nuclease, and detergents reveal encasement

within double-layered membrane compartments. J. Biol. Chem. 278:24388–24398.
59. Wang, S. H., W. J. Syu, K. J. Huang, H. Y. Lei, C. W. Yao, C. C. King, and S. T. Hu. 2002. Intracellular localization and determination of a nuclear localization signal of the core protein of dengue virus. J. Gen. Virol. 83: 3093–3102.
60. Wang, Y., M. Lobigs, E. Lee, and A. Mullbacher. 2003. CD8$^+$ T cells mediate recovery and immunopathology in West Nile virus encephalitis. J. Virol. 77: 13323–13334.
61. Westaway, E. G., A. A. Khromykh, M. T. Kenney, J. M. Mackenzie, and M. K. Jones. 1997. Proteins C and NS4B of the flavivirus Kunjin translocate independently into the nucleus. Virology 234:31–41.
62. Wurm, T., H. Chen, T. Hodgson, P. Britton, G. Brooks, and J. A. Hiscox. 2001. Localization to the nucleolus is a common feature of coronavirus nucleoproteins, and the protein may disrupt host cell division. J. Virol. 75: 9345–9356.
63. Yamshchikov, V. F., and R. W. Compans. 1994. Processing of the intracellular form of the West Nile virus capsid protein by the viral NS2B-NS3 protease: an in vitro study. J. Virol. 68:5765–5771.
64. Yang, K. D., W. T. Yeh, R. F. Chen, H. L. Chuon, H. P. Tsai, C. W. Yao, and M. F. Shaio. 2004. A model to study neurotropism and persistency of Japanese encephalitis virus infection in human neuroblastoma cells and leukocytes. J. Gen. Virol. 85:635–642.

JOURNAL OF VIROLOGY, Jan. 2005, p. 1271–1281 Vol. 79, No. 2
0022-538X/05/$08.00+0 doi:10.1128/JVI.79.2.1271–1281.2005


# Molecular Determinants for Subcellular Localization of Hepatitis C Virus Core Protein

Ryosuke Suzuki,[1] Shinichiro Sakamoto,[1] Takeya Tsutsumi,[1] Akiko Rikimaru,[1,2] Keiko Tanaka,[3] Takashi Shimoike,[1] Kohji Moriishi,[4] Takuya Iwasaki,[3,5] Kiyohisa Mizumoto,[2] Yoshiharu Matsuura,[4] Tatsuo Miyamura,[1] and Tetsuro Suzuki[1]*

*Department of Virology II, National Institute of Infectious Diseases, Shinjuku-ku,[1] Department of Biochemistry, School of Pharmaceutical Sciences, Kitasato University, Minato-ku,[2] and Department of Pathology, National Institute of Infectious Diseases, Shinjuku-ku,[3] Tokyo, Research Center for Emerging Infectious Diseases, Research Institute for Microbial Diseases, Osaka University, Suita-shi, Osaka,[4] and Department of Pathology, Institute of Tropical Medicine, Nagasaki University, Nagasaki-shi, Nagasaki,[5] Japan*

Received 21 June 2004/Accepted 26 July 2004

**Hepatitis C virus (HCV) core protein is a putative nucleocapsid protein with a number of regulatory functions. In tissue culture cells, HCV core protein is mainly located at the endoplasmic reticulum as well as mitochondria and lipid droplets within the cytoplasm. However, it is also detected in the nucleus in some cells. To elucidate the mechanisms by which cellular trafficking of the protein is controlled, we performed subcellular fractionation experiments and used confocal microscopy to examine the distribution of heterologously expressed fusion proteins involving various deletions and point mutations of the HCV core combined with green fluorescent proteins. We demonstrated that a region spanning amino acids 112 to 152 can mediate association of the core protein not only with the ER but also with the mitochondrial outer membrane. This region contains an 18-amino-acid motif which is predicted to form an amphipathic α-helix structure. With regard to the nuclear targeting of the core protein, we identified a novel bipartite nuclear localization signal, which requires two out of three basic-residue clusters for efficient nuclear translocation, possibly by occupying binding sites on importin-α. Differences in the cellular trafficking of HCV core protein, achieved and maintained by multiple targeting functions as mentioned above, may in part regulate the diverse range of biological roles of the core protein.**

Hepatitis C virus (HCV), the most important causative agent of posttransfusion and sporadic non-A, non-B hepatitis, is a positive-stranded RNA virus belonging to the family *Flaviviridae* (7). A precursor polyprotein of about 3,000 amino acids is encoded by a large open reading frame of the genome and undergoes cellular and viral protease-mediated posttranslational modification to produce a series of structural and nonstructural proteins (8, 13, 16).

HCV core protein, which is derived from the N terminus of the viral polyprotein, forms multimers and interacts physically with the viral RNA to constitute the nucleocapsid (28, 47, 50). Tissue transglutaminase is responsible for stabilizing the core protein by cross-linking it into a dimeric form (26). In addition, the core viral protein has properties which enable it to modulate a number of cellular processes, including transcription, inhibition or stimulation of apoptosis, and suppression of host immunity, as reviewed previously (21, 29, 51, 52). Several studies suggest that expression of the core protein affects mitochondrial function and lipid metabolism. The core protein increases the cellular production of reactive oxygen species with subsequent increases in lipid peroxidation (35, 39). The viral protein also colocalizes with human apolipoprotein AII, associates with lipid droplets, and has the capacity to influence metabolic events involving lipid storage (2, 17, 30, 36, 44). In addition, the core protein reduces microsomal triglyceride transfer, leading to defects in very low density lipoprotein assembly and secretion (40). Furthermore, the HCV core protein has transforming potential in some cells under certain conditions (5, 42). Transgenic mice expressing this protein in the liver develop hepatic steatosis due to increased oxidative stress in the absence of inflammation, with subsequent development of hepatocellular carcinoma (34, 36). These results suggest that the HCV core protein might play a pivotal role in the pathogenesis of hepatitis C in addition to its role as a structural component of the viral capsid.

The amino acid sequence of the core protein is well conserved among different HCV isolates and genotypes compared to other HCV proteins. The N-terminal domain of the HCV core protein is highly basic, while its C terminus is hydrophobic. Although several core proteins of various sizes exist (17 to 23 kDa) (15, 23, 25, 49, 56), two processing events result in the predominant production of a 21-kDa core protein. Both of these events utilize the endoplasmic reticulum (ER). The first one is to be cleaved from downstream envelope protein E1 at position 191, where the C-terminal hydrophobic domain serves as a putative signal peptide sequence. Subsequently, the signal sequence of 13 or 18 residues is processed by signal peptide peptidase (19, 23, 56).

The HCV core protein is found primarily within the membranes of cytoplasmic organelles, but it is also found in the nucleus (23, 48, 56). Immunofluorescence studies show a punc-

* Corresponding author. Mailing address: Department of Virology II, National Institute of Infectious Diseases, 1-23-1 Toyama, Shinjuku-ku, Tokyo, Japan 162-8640. Phone: (81) 3-5285-1111. Fax: (81) 3-5285-1161. E-mail: tesuzuki@nih.go.jp.

tate pattern, consistent with ER localization, as well as perinuclear localization (15, 24, 32, 46, 56). Some studies suggest direct effects of the core protein on mitochondrial function. In fact, the core protein localizes to the mitochondria (34, 39). The N-terminal domain of the core protein contains three stretches of arginine- and lysine-rich sequences. Translocation of the core protein to the nucleus, mediated by these basic-residue stretches which function as nuclear localization signals (NLSs), is observed (6, 48). In addition, Moriishi et al. demonstrated that the N-terminal region of the core protein is also essential for nuclear retention through its interaction with the proteasome activator PA28γ (33).

In this study, we found a region that is important for localization of the mature core protein to the ER and to the mitochondrial outer membrane. We also identified a novel bipartite NLS responsible for nuclear targeting of the core protein, presumably via an importin-dependent pathway.

## MATERIALS AND METHODS

**Plasmid construction.** The construction of a plasmid expressing the full-length core protein of 191 amino acids, pCAGC191, was described previously (49). pGFP, a construct expressing green fluorescent protein (GFP) with a C-terminal Myc epitope tag sequences, was prepared as follows. pCMV/Myc/mito/GFP (Invitrogen Corp., Carlsbad, Calif.) was digested with PmlI, followed by treatment with the Klenow fragment of DNA polymerase I. The resultant linear fragment was ligated to a PstI linker (GCTGCAGC) and digested with PstI to remove the mitochondrial targeting signal sequence, followed by self-ligation. A series of HCV core-GFP fusion constructs were made by amplifying the core gene fragments with PCR with primers containing Flag epitope tag sequences (sense) and a PstI site (both). After digestion with PstI, the segments were inserted into the PstI site of pGFP. A series of GFP-core-E1 fusion constructs were made by amplifying core and E1 gene fragments with PCR with primers containing a NotI site. After digestion with NotI, the segments were inserted into the NotI site of pGFP.

pGEX-4T-1 (Amersham Bioscience Corp., Piscataway, N.J.) was used to express core protein fused with glutathione *S*-transferase (GST) in *Escherichia coli*. Core cDNA fragments encoding amino acids 1 to 71 were inserted into the EcoRI site of pGEX-4T-1. Alanine substitutions were introduced into the core protein by PCR mutagenesis with primers containing base alterations. The PCR products were then cloned into pCR2.1 (Invitrogen Corp.) and verified by DNA sequencing. Individual cDNAs were excised and inserted separately into pGFP or pGEX-4T-1. The primer sequences used in this study are available from the authors upon request.

Plasmid pRSET-hSRP1α (54), containing importin-α cDNA under the control of a T7 promoter, was kindly provided by Karsten Weis (University of California, Berkeley). A cDNA clone of importin-α possessing 14 residues (MYPYDVP DYGGGGS), derived in part from the hemagglutinin (HA) tag at the N terminus, was constructed by PCR. The resultant linear fragment was inserted under the control of a CAG promoter of pCAGGS and designated pCAG-HA-imp.

**Cell culture and transfection.** Human embryonic kidney 293T cells were maintained in Dulbecco's modified Eagle's medium supplemented with 100 units of penicillin per ml, 100 μg of streptomycin per ml, and 10% fetal bovine serum at 37°C in a 5% $CO_2$ incubator. Monolayers of 293T cells were transfected with plasmid DNA in the presence of Lipofectamine (Gibco-BRL, Life Technologies, Gaithersburg, Md.) according to the manufacturer's instructions.

**Confocal immunofluorescence microscopy.** Transfected cells were grown on glass coverslips. Two days after transfection, cells were fixed with 4% paraformaldehyde in phosphate-buffered saline (PBS) for 20 min at room temperature. Intracellular localization of HCV core-GFP fusion proteins was visualized in cells transfected with a variety of GFP fusion constructs.

In order to detect the HCV core protein by immunofluorescence, fixed cells were permeabilized with 0.2% Triton X-100 in PBS for 3 min at room temperature, followed by blocking with a nonfat milk solution (Block Ace; Snow Brand Milk Products Co., Sapporo, Japan). The cells were then incubated with anticore monoclonal antibody B2 (Anogen, Mississauga, Canada) for 60 min at room temperature, followed by incubation with fluorescein isothiocyanate-conjugated rabbit anti-mouse immunoglobulin G (IgG) (ICN Pharmaceuticals, Aurora, Ohio) for 45 min. To visualize mitochondria, MitoTracker Red CM-$H_2$XRos (Molecular Probes, Eugene, Oreg.) was added to the culture medium to a final concentration of 100 nM and incubated for 120 min at 37°C prior to fixation. To visualize the ER, goat anticalregulin antibody (Santa Cruz Biotechnology, Santa Cruz, Calif.) and rhodamine-conjugated rabbit anti-goat IgG (ICN Pharmaceuticals) were used as the first and second antibodies, respectively. To visualize HA-importin-α, mouse anti-HA antibody (Roche Molecular Biochemicals, Indianapolis, Ind.) and rhodamine-conjugated goat anti-mouse IgG (ICN Pharmaceuticals) were used as the first and second antibodies, respectively. All specimens were examined with an LSM510 laser scanning confocal microscope (Carl Zeiss, Oberkochen, Germany).

**Immunoelectron microscopy.** Cells were transfected as described above. After 2 days, cells were fixed with 3% paraformaldehyde and 0.1% glutaraldehyde in 0.1 M PBS (pH 7.4). Free aldehyde groups were quenched with 50 mM $NH_4Cl$ in PBS. The cell pellets were embedded at progressively lower temperatures (down to −35°C) in Lowicryl k4M according to an established protocol (43). Ultrathin sections were prepared and mounted on carbon-coated nickel grids. To perform electron microscopy, Lowicryl k4M ultrathin sections, mounted on grids, were floated on a droplet of PBS containing 1% bovine serum albumin, 0.1% Triton X-100, and 0.1% Tween 20 for 10 min, after which they were exposed to droplets of mouse anticore monoclonal antibody (Anogen) diluted in PBS for 45 min. Following this, they were rinsed twice for 5 min each in PBS and incubated with anti-mouse IgG-coated 10-nm immunogold particles (British Biocell, Cardiff, United Kingdom) for 45 min. After rinsing with PBS and distilled water, the grids and embedded sections were air dried and exposed to uranyl and lead acetate contrast agents.

**Subcellular fractionation.** All steps were performed at 4°C in the presence of a protease inhibitor cocktail called Complete (Roche Molecular Biochemicals). To isolate the ER fraction, transfected cells were washed with PBS, lysed in homogenization buffer A (50 mM Tris-HCl [pH 8.0], 1 mM β-mercaptoethanol, 1 mM EDTA, and 0.32 M sucrose), and then centrifuged at 5,000 × *g* for 10 min. The supernatant was then collected and centrifuged at 105,000 × *g* for 1 h. The pellet was disrupted in lysis buffer (50 mM Tris-HCl [pH 7.5], 150 mM NaCl, 1% NP-40, 1 mM dithiothreitol, 1 mM sodium orthovanadate, and 10 mM sodium fluoride), after which it was centrifuged at 15,000 × *g* for 20 min. The resulting supernatant was used as the ER fraction.

To isolate the mitochondrial fraction, transfected cells were washed with PBS and homogenized in ice-cold homogenization buffer B (200 mM mannitol, 50 mM sucrose, 1 mM EDTA, and 10 mM Tris-HCl) at pH 7.4. The supernatant was then centrifuged at 1,000 × *g* for 10 min to remove large debris and nuclei. The resulting supernatant was then centrifuged at 20,000 × *g* for 20 min to obtain crude mitochondria. The crude mitochondria pellet was subfractionated in Nycodenz gradients for further purification of mitochondria. Nycodenz (Axis-Shield PoC AS, Oslo, Norway) solution at 50% (wt/vol) was prepared in buffer containing 5 mM Tris-HCl and 1 mM EDTA at pH 7.4. This stock solution was then diluted with buffer containing 0.25 M sucrose, 5 mM Tris-HCl, and 1 mM EDTA at pH 7.4 before use. The crude mitochondrial pellets was suspended in 4 ml of 25% Nycodenz solution and overlaid onto the following discontinuous Nycodenz gradients: 1 ml of 40%, 1 ml of 34%, and 2 ml of 30%. The samples were topped off with 2 ml of 23% Nycodenz solution after placement onto the discontinuous gradients. The tubes were then centrifuged at 52,000 × *g* for 90 min. The dense band seen after centrifugation at the 25 to 30% interface was recovered as the purified mitochondrial fraction.

To determine the submitochondrial localization pattern of the core protein, mitochondria were resuspended in SH buffer (0.6 M sorbitol and 20 mM HEPES-KOH [pH 7.2]) in the absence or presence of 30 μg of proteinase K per ml after purification by Nycodenz density gradient centrifugation. Samples were incubated for 30 min at 0°C, after which protease digestion was halted by the addition of *p*-aminophenyl methanesulfonyl fluoride hydrochloride (*p*-APMSF) (5 mM). Proteins lysed in sodium dodecyl sulfate (SDS) sample buffer were analyzed by SDS-polyacrylamide gel electrophoresis (PAGE) and immunoblotted as described below.

**Immunoblot analysis.** The proteins were transferred to a polyvinylidene difluoride membrane (Immobilon; Millipore, Tokyo, Japan) after separation by SDS-PAGE. After blocking, the membranes were probed with monoclonal- or polyclonal-antibody against core protein (Anogen), prohibitin (Neo Markers, Fremont, Calif.), ribophorin I (Santa Cruz Biotechnology), translocase of the outer membrane (Tom) 20 (Santa Cruz Biotechnology), translocase of the inner membrane (Tim) 17 (Santa Cruz Biotechnology), or GFP (Santa Cruz Biotechnology). Immunoblots were developed as previously described (15).

**GST pulldown assay.** *Escherichia coli* BL21 cells were transformed with GST-core fusion plasmids and grown at 37°C. Expression of the fusion protein was induced by 1 mM isopropyl-β-D-thiogalactopyranoside at 37°C for 3 h. Bacteria were harvested, suspended in lysis buffer (1% Triton X-100 in PBS), and soni-

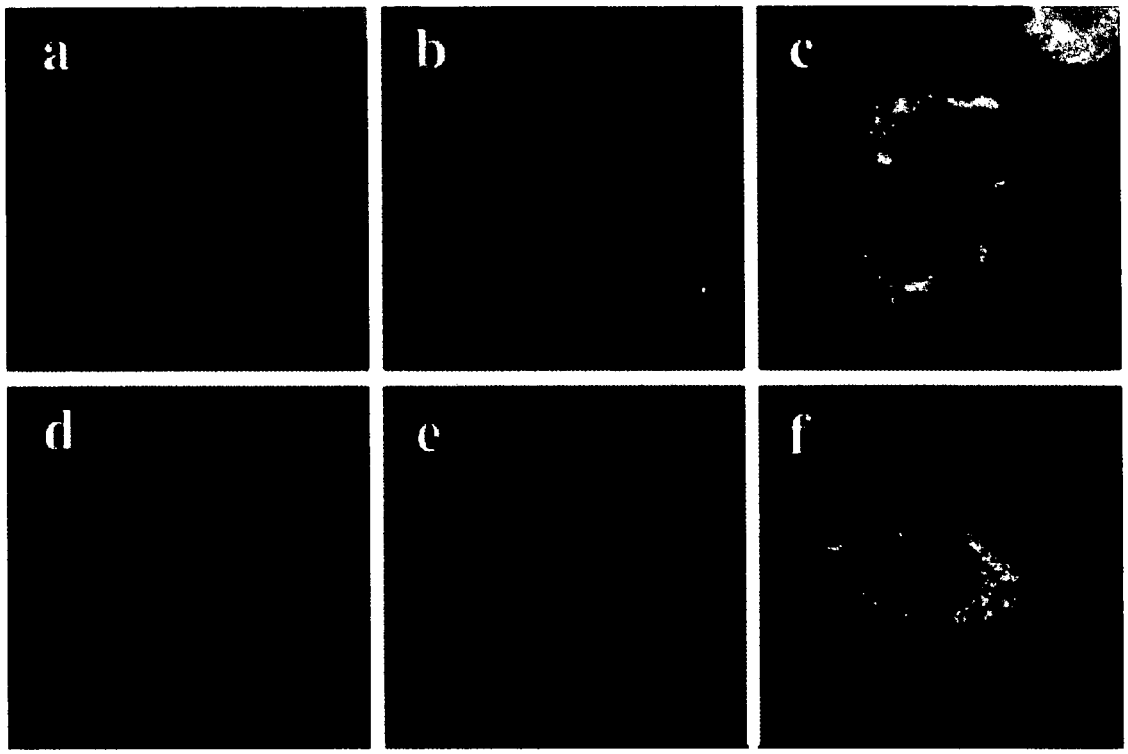


FIG. 1. Confocal analysis of double staining for HCV core protein and ER or mitochondria. 293T cells transfected with full-length HCV core expression plasmid, pCAGC191 were allowed to express the plasmid for 2 days. Transfected cells were fixed directly (a to c) or fixed after loading with Mitotracker (d to f). After permeabilization with Triton X-100, cells were subjected to immunofluorescence staining with a mouse anticore antibody. A goat anticalregulin antibody was used for ER staining. The green signals corresponding to the core were found with a fluorescein isothiocyanate-conjugated rabbit anti-mouse IgG (a and d). The red signals corresponding to the ER were obtained with a rhodamine-conjugated rabbit anti-goat IgG secondary antibody (b). Mitochondria were stained with the mitochondrion-selective dye Mitotracker (e). Overlay resulted in yellow signals indicative of colocalization (c and f).

cated on ice. GST and GST fusion proteins were purified from bacterial lysates with glutathione-Sepharose beads (Amersham Bioscience Corp.). The beads were washed four times with lysis buffer. Approximately equal amounts of purified protein, as estimated by Coomassie brilliant blue staining, were used for the binding assays. For pulldown assays, in vitro transcription and translation of importin-α was done with pRSET-hSRP1α and the TNT-coupled reticulocyte lysate system (Promega Corp., Madison, Wis.) with T7 RNA polymerase. The reaction was carried out at 30°C for 4 h in the presence of [$^{35}$S]methionine/cysteine (ICN Pharmaceuticals). The translation product was then incubated with glutathione-Sepharose beads bound to GST fusion proteins in 1 ml of binding buffer (40 mM HEPES [pH 7.5], 100 mM KCl, 0.1% NP-40, and 20 mM 2-mercaptoethanol) at 4°C for 1 h. The beads were washed four times with binding buffer, and the pulldown complexes were separated by SDS-PAGE on 15% polyacrylamide gels. The gels were then fixed, dried, and analyzed with autoradiography.

## RESULTS

**Subcellular localization of HCV core protein.** To assess the subcellular localization of HCV core protein, we first analyzed cells transfected with a full-length core-expressing construct by confocal microscopy. In accordance with previous observations (2, 15, 32, 45, 56), a granular cytoplasmic staining pattern of the core protein was observed in 293T (Fig. 1) and human hepatoblastoma HepG2 (data not shown) cells. Dual staining of transfected cells with antibody against the ER protein calregulin along with anticore antibody confirmed the ER localization of the core protein (Fig. 1a, b, and c show the core,

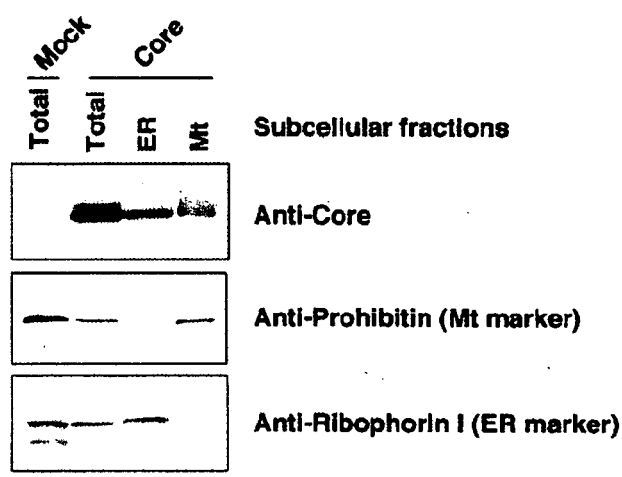


FIG. 2. Subcellular distribution of HCV core protein analyzed by immunoblotting. ER and mitochondrial (Mt) fractions were isolated from 293T cells expressing the full-length core protein (Core) or nontransfected cells (Mock) 2 days after transfection. Equal amounts of protein from each fraction as well as whole cell lysates (Total) were subjected to immunoblotting with a monoclonal antibody against either HCV core, prohibitin, or ribophorin I.